# An evaluation of the effects of PDMS-based PDL on a Ti dental implant using FEM

## Renan de Freitas Inocente

Dissertation presented to the School of Technology and Management of the Polytechnic Institute of Bragança to obtain a Master's Degree in Industrial Engineering, Mechanical Engineering branch, under the double degree with the Federal Technological University of Paraná campus Cornélio Procópio.

Work oriented by:

Professor PhD João Eduardo Ribeiro

Professor PhD Luís Ribeiro de Mesquita

Professor PhD Julio Cesar de Souza Francisco

Bragança

2020-2021

# An evaluation of the effects of PDMS-based PDL on a Ti dental implant using FEM

## Renan de Freitas Inocente

Dissertation presented to the School of Technology and Management of the Polytechnic Institute of Bragança to obtain a Master's Degree in Industrial Engineering, Mechanical Engineering branch, under the double degree with the Federal Technological University of Paraná campus Cornélio Procópio.

Work oriented by:

Professor PhD João Eduardo Ribeiro

Professor PhD Luís Ribeiro de Mesquita

Professor PhD Julio Cesar de Souza Francisco

Bragança

2020-2021

# Acknowledgement

# Abstract

PDMS is a polymer with hyperelastic characteristics that have different qualities and numerous applications. Its use in the industry gradually increases every year, some sectors that can be cited as the most important are automotive, aeronautics, and biomechanics. Because it is colorless, inert, odorless, biocompatible, and with mechanical properties to some tissues of the human body, its use in biomechanics, more specifically in odontology, is inherent.

The vast majority of dental implants are made of titanium, a material that despite being biocompatible, has mechanical properties incredibly superior to cortical bone, medullary, and even natural teeth. This makes it difficult for the implant to do its job properly, as it would absorb minimal amounts of energy. Thus putting great stress on the jawbones, can cause discomfort, rejection, premature failure, among others.

After the removal of a natural tooth, the periodontal ligament (PDL), which is a soft film around the tooth root, is lost. It has fundamental functions, as it is elastic, partially absorbs the mechanical energy deposited on the tooth crest, increases the area of contact with the bone, and protects it. Therefore, the objective of this work is to numerically simulate a PDMS film replacing the lost PDL.

The present work studied a PDMS film as a substitute form of PDL. The data referring to the PDMS were taken from tensile tests and other materials by the theoretical framework. The simulations performed by FEM create hypothetical situations that the implant with and without film would face to study its behavior.

Therefore, this project verified that the PDMS reduced the stresses in the implant, for the abutment had a momentary increase in stress even when there is contact with the

crown, then it reduces the stress growth rate, both expected behaviors. It acted similarly to the periodontal ligament in terms of tension distribution in the bone, it was observed that even maintaining maximum stress, it is more dispersed and relocated to the fundus, instead of the crest.

The results of this project are only linked to the studied geometry, another implant would probably present other results. Therefore, it is not possible to state that PDMS is a definitive replacement for PDL, but indicates that it is a candidate.

# Resumo

O PDMS é um polímero com características hiperelásticas que apresenta diversas qualidades e com inúmeras aplicações. Sua utilização na indústria aumenta gradualmente todos os anos, alguns setores que podem ser citados como os mais importantes são automobilístico, aeronáutico e biomecânico. Por ser incolor, inerte, inodoro, biocompatível e com propriedades mecânicas a alguns tecidos do corpo humano, sua utilização na biomecânica, mais especificamente na odontologia é inerente.

A grande maioria dos implantes dentários é feita de Titânio, um material que apesar de ser biocompatível, possui propriedades mecânicas incrivelmente superiores ao osso cortical, medular, e até o dente natural. Isto dificulta o implante de realizar seu trabalho apropriadamente, visto que absorveria quantidades mínimas de energia. Assim passando grandes tensões aos ossos da mandíbula, pode causar desconforto, rejeição, falha prematura entre outros.

Após a retirada de um dente natural, o ligamento periodontal (LPD), que é uma película macia envolta a raiz do dente, é perdido. Tem funções fundamentais, como é elástica, absorve parcialmente energia mecânica depositada na crista do dente, aumenta a área de contato com o osso e o protege. Sendo assim, o objetivo deste trabalho é simular numericamente uma película de PDMS substituindo o perdido LPD.

O presente trabalho estudou uma pelicula de PDMS como forma substirutiva do LPD. Os dados referentes ao PDMS foram retirados de ensaios de tração e dos outros materias pelo referencial teórico. As simulações realizadas por MEF criam situações hipotéticas que o implate com e sem pelicula enfrentaria afim de estudar seu comportamento.

Diante disso, este projeto verificou que de fato o PDMS reduziu as tensões no implante,

para o pilar teve um aumento momentâneo de tensão até quando há contato com a coroa, depois reduz a taxa de crescimento de tensão, ambos comportamentos esperados. Agiu similarmente ao ligamento periodontal em termos de distribuição de tensão no osso, observou-se que mesmo mantendo a tensão máxima, está mais dispersa e realocada ao fundo, ao invés da crista.

Os resultados deste projeto estão unicamente vinculados a geometria estudada, outro implante provavelmente apresentaria outros resultados. Portanto não é possível afirmar que o PDMS é um substituto definitivo do LPD, mas indica que é um candidato.

**Palavras-chave:** Ligamento Periodontal (LPD); Método de Elementos Finitos (MEF); Titânio (Ti); Implante dentário; Polidimetilsiloxano (PDMS).

# Contents

# List of Abbreviations and Symbols

The next list describes nomenclatures that will be later used within the body of the document.

$A_0$            Initial Cross Sectional Area

Al            Aluminium

CNC            Computer Numerical Control

$\Delta$            Variation

E            Modulus of Elasticity or Young's Modulus

$\varepsilon$            Deformation

FEM            Finite Elements Method

F            Force

$F_{sf}$            Static Friction Force

IPB            Polytechnic Institute of Bragança

$l$            Length

$l_0$            Initial Length

LPD            Ligamento Priodontal

MEF            Método de Elementos Finitos

| | |
|---|---|
| $\mu_s$ | Static Friction Coefficient |
| N | Normal Force |
| PDL | Periodontal Ligament |
| PDMS | Polydimethylsiloxane |
| $\sigma$ | Stress |
| $\sigma_{ult}$ | Ultimate Tensile Strength |
| $\sigma_{yield}$ | Yield Tensile Strength |
| SI | International System of Units |
| Ti | Titanium |
| UTFPR-CP | Federal Technological University of Paraná campus Cornélio Procópio |
| V | Vanadium |

# List of Tables

# List of Figures

# Chapter 1

# Introduction

There have been many innovations and studies developed that seek to mitigate or even propose definitive solutions in the human body, whether these, from components related to locomotion or more complex, such as those that comprise neural regions, that is, extremes that allow us to understand the whole involvement of biological and biomechanical areas that together are essential for those advances.

In general, biomechanics can be defined as the science that examines the forces and effects acting on and within a human structure, a description that presented to the field of dentistry fits perfectly into the way of interpreting and understand the structural behavior of the set that make up a dental implant [1].

Biomechanics can be approached as the way to analyze the interactions of implant and bone, in addition to studying the distribution of loads incident on implant-supported prostheses in the different situations in which the dental implant is used for the replacement of missing teeth. In addition to an aesthetic condition, dental implants aim to provide comfort and functionality to the patient, transmit security and confidence when consuming foods that require more effort [2].

It is a promising market, in 2019 alone, 2.7 million implants were sold in Brazil. The market cap in 2020 was USD 3.66 billion worldwide, and is expected to reach USD 5.71 billion by 2028. The rise of the sector follows the significant growth of the elderly population [3]. The number of people who use some type of dental prosthesis in the Brazil,

according to a survey by the Brazilian Institute of Geography and Statistics (IBGE), is one in five people having between 25 and 44 years old and the rest above 45.

Therefore, it is necessary to constantly strive for new proposals for increasingly efficient dental systems, aiming at quality and perfection, since poorly designed implants could cause irreversible damage, cause failures in rehabilitation and exceed the physiological limit causing loss of osseointegration, which is the stable and functional union between the bone and the implant surface. Besides causing discomfort to the patient, considering that it is a sensitive region and used very often for food, it can easily cause injuries and, consequently, pain and even infections.

Regardless of the cause, removing a natural tooth from the root will result in the loss of the periodontal ligament (PDL). This viscous substance has several peculiar characteristics that alter the behavior of the system. It is possible to highlight the absorption of mechanical energy deposited on the tooth crest. Without it, there can be a compromise in the system's behavior in general. Most of the implants does not have any kind of PDL.

Polydimethylsiloxane (PDMS) is a silicone elastomer, and is currently one of the most used organic polymeric materials in the biomedical industry due to its numerous characteristics, namely biocompatibility, low cost, easily handled at room temperature, colorless, inert, odorless, and mechanical properties similar to some tissues of the human body. Its use in biomechanics, more specifically in odontology, is inherent.

Although it is an area that is only likely to grow and move a lot of money, it still requires some improvements, such as increasing the absorption of mechanical energy by the implant to produce better patient experiences. Hence, the goal of this research is to evaluate the application of PDMS film as a PDL substitute to a titanium dental implant.

## 1.1   Objectives

### 1.1.1   Main Objective

- Study the behavioral influence of a PDMS film surrounding a Ti dental implant to validate its use as substitute for the PDL lost.

### 1.1.2   Specific Objectives

- Produce the PDMS specimen, do the tensile tests, and handle the data of the test;

- Simulate the tensile test, and the implant in various cases with FEM and compare themselves.

## 1.2   Document Structure

The first chapter showed the introduction and the motivation reasons for the project's existence. There is possible to find general data that show how big this area is and its potential, and the objectives this work is trying to achieve.

As expected, the second chapter will show every scientific argument used to establish this paper correctly. It is possible to find information about: natural teeth, periodontal ligaments, dental implants, preload, osseointegration, loading, PDMS, and friction. The third chapter will show the exact procedure the author did to accomplish this paper, from the creation of the specimen until the last implant simulation.

For chapter four, the results and their discussion will be presented. All the useful information of the expected results and the actual results and discussions of the project and its process.

Finally, chapter five consists of conclusions, final considerations, limitations faced, accomplishments, and the possibility of future works.

# Chapter 2

# Theoretical Foundations

## 2.1   Natural Teeth

Mammalian teeth are heavily used working tools made to reduce and grind food so it can be further processed by the intestine. They usually have a crown consisting of one or more cusps that protrude into the oral cavity, and one or more roots that anchor the teeth to the jaw, through a specialized ligament fixation in the system [4].

The outer regions of the crown consist of a hard, wear-resistant layer of highly mineralized enamel covering a dentin core bone. The roots are also made of dentin and are coated with cementum, which is a low-density bone tissue [5].

The adult human body has 32 permanent teeth. The natural structure of the teeth, as mentioned above, is shown in Figure 2.1.
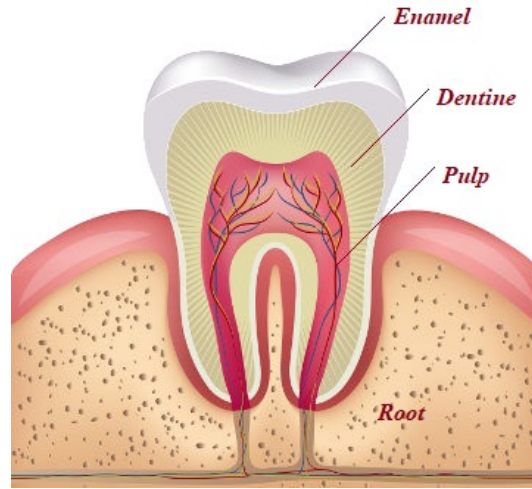
Figure 2.1: Natural Tooth Structure.

The teeth are connected to the maxillary bone through cementum and through a thin membrane, the periodontal ligament (PDL), which will be better explained in the next topic, made of collagen fibers surrounded by a gel-like matrix of proteoglycans and cells. The compatible nature of the PDL allows for some mobility of the teeth in their orbits [6].

Forces crush food and any excess deformation energy that is not consumed by comminution is distributed through the crown and roots. This leads to deformation of the PDL and, consequently, dissipation in the supporting tissues [7][8].

Maximum reported chewing loads for common foods measured in human molars are between 70 N and 150 N, based on direct measurements in human volunteer teeth [9][10].

When analyzing the efforts supported by the teeth, the oblique and lateral forces spread along the upper surface of the teeth, called the bone crest, and go towards the apex, which is found at the end of the root of the teeth. A natural tooth can move from 56 to 108 $\mu$m and rotate towards the apex, minimizing the resulting load on the bone crest. Therefore, the tooth will always seek an adaptation that will reduce the load on the bone crest [11].

In Figure 2.2, through a finite element analysis it is possible to verify what was mentioned by Misch in 2006, analyzing the effect of the bite, which is the occlusal contact,

it is possible to observe the distribution of forces on the teeth, due to the biomechanical characteristics of the dental tissues, the stresses are distributed along the axis of the teeth, from the crest to the apex [11].
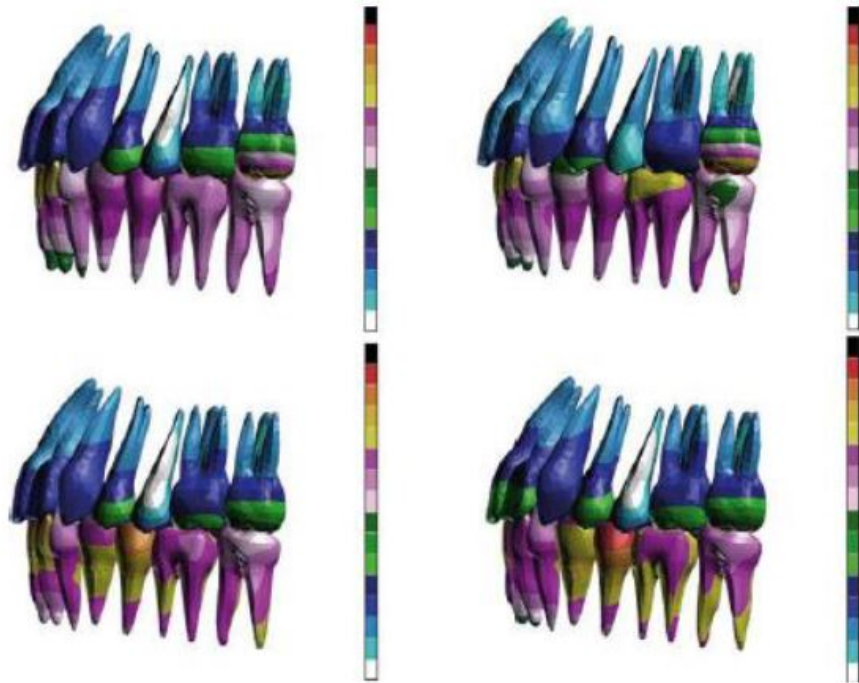


Figure 2.2: Finite element analysis demonstrating the distribution of forces in teeth [12].

Natural teeth are wider than implants, which often cannot be larger, because the pre-existing bone volume is limited. This is relevant since the magnitude of stress transmitted to the surrounding bone is inversely proportional to the width of the trans-osseous structure, which means that the greater the width of the tooth, the less stress suffered to the surrounding bone [11].

## 2.2  Periodontal ligament

There is a soft connective tissue union between bones and teeth called the periodontal ligament (PDL). PDL is composed of several types of collagen and has a component neurovascular function. It is extremely thin, but very complex. It is embedded in the

bone around the tooth and also in the outer layer of the root, called the cementum [13].

The periodontal ligament is found only between the root tooth and adjacent bone and does not support the outer gingival tissue. The ligament also understands the movement of the tooth and helps them to grow. This complex tissue allows the tooth to function under the load of chewing and absorbs excess pressure resulting from bruxism [14].

If there was no such tissue and the tooth was connected directly to the bone, it would work like an implant and could not be moved. Furthermore, as the tooth is corrected in the socket by the periodontal ligament and not by a direct interface between the bone, it is possible to extract it, in most cases, without removing small areas of the alveolar bone [14].

Tooth enamel is an inert and therefore insensitive tissue, but the periodontal ligament is innervated by autonomic and sensory nerve fibers, the former carrying vasomotor information and the latter carrying nociceptive and proprioceptive information [4].

Its ability to generate important proprioceptive information in mastication control is of interest to neurophysiologists. However, the study of the periodontal ligament should not be limited to those involved only in dental research. The periodontal ligament has properties that make it a particularly useful model for investigating problems associated with soft fibrous connective tissue [6].

The periodontal ligament has much in common with soft connective tissue elsewhere in the body. In addition, it has other features, which are somewhat unusual. An appreciation of their many characteristics can provide the basis for a greater understanding of their biological behavior. One factor to keep in mind when reviewing research on the periodontal ligament is that most researchers use animal material [6].

Like all soft fibrous connective tissues, the periodontal ligament consists of a fibrous stroma in a ground substance gel containing cells, blood vessels, and nerves. The fibrous stroma consists mainly of collagen (with small amounts of oxitalan) and the cells are mainly fibroblasts [6].

The main constituent of this structure are collagen fibers, called Sharpey fibers, divided into groups according to their orientation and insertion. The main functions of

the periodontal ligament are, in addition to supporting the tooth in the socket and the sensory function, due to its abundant innervation, the transmission of occlusal forces to the supporting alveolar bone, cell formation and nutrition, as well as the cement and the gum [15].

The periodontal ligament consists primarily of fiber-rich connective tissue that support the tooth in the socket and keep it attached to the alveolar bone. Collagen represents approximately 50% of the weight of the entire periodontal ligament. The organization of these collagen fibers: fibers that passed directly from the tooth to the bone, called main fibers. Later, it was proposed that the main fibers did not pass directly from the tooth to the bone, with junction sites in the middle of the ligament [15].

It is suggested that the intermediate plexus was a histological artifact that arises as a result of the oblique sectioning plane. However, the periodontal ligament fibers can be studied with scanning electron microscopy, which allows classifying the main fibers into several groups: 1) Alveolar crest group, from the alveolar crest to the cervical region of the root; 2) Horizontal group, consisting of horizontal fibers that extend from the tooth to the alveolar bone; 3) Oblique group, obliquely oriented fibers with insertion into the cementum. There is a greater amount of these fibers in the occlusal region of the alveolar bone, making up two-thirds of the total number of fibers in this region. 4) Apical group, fibers that spread from the apex of the tooth to the bone [16].

Collagen fibers are designed to withstand the forces applied to the teeth. Studies have shown that Sharpey's fibers, both in alveolar bone and in cellular cementum, end up in the form of a non-calcified nucleus, surrounded by a calcified sheath. In 1977, the trajectory of fibers between adjacent teeth was studied in sections of monkey mandibles stained with silver nitrate. He observed in the interseptal bone, periods of bone resorption and apposition, while there was loss of collagen fibers to form new fibers [17].

## 2.3　Dental Implants

Dental implants help to replace the tooth root in addition to supporting the prosthesis, contributing to a better physical appearance and chewing function, world leading swiss implantology company, they are indicated for patients with unitary, partial or all teeth loss [18].

　　As mentioned in the previous chapter, the structure of a dental implant can be composed of three parts: crown, retention screw and implant, which is introduced into the medullary bone, as shown in Figure 2.3.

　　To represent the chewing load, an oblique force of 133 N was considered inclined at 30° with the vertical and displaced 2 mm from the axis of the implant [12].

　　As it is a symmetrical model, only half of the 3D model will be considered for this study, attributing the orthogonal restrictions on the cut face, as well as to simulate the real conditions, restrictions in x and y were attributed to the cortical and medullary bone and only in x for implant, crown and screw.

　　For these analyses, the Ansys pre- and post-processor was used, as well as to generate the model of the three-dimensional finite elements of 3D meshes.
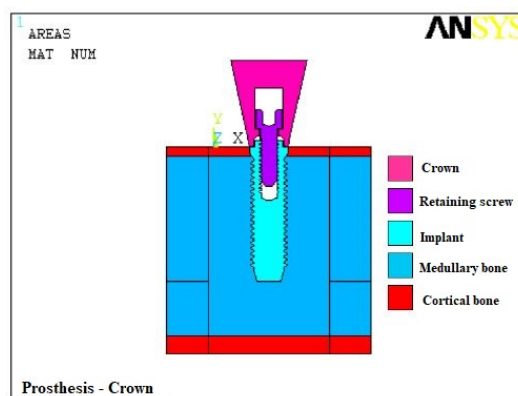


Figure 2.3: Biomechanical model with highlighted contact areas [12].

　　The more the modulus of elasticity of the implant resembles that of adjacent biological tissues, the lower the probability of relative movement in the tissue/implant interface. The

comparison between the materials can be seen in Table 1 below. The cortical bone, into which the implant is inserted, is at least five times more flexible than titanium [19].

The reason why it is possible to replace the natural tooth with the dental prosthesis, but at low tensions, is the proportionality of the tension and the relative difference between bone and titanium rigidity, so as the intensity of tension decreases, the relative difference between bone and titanium stiffness also decreases [19].

Among the materials used, the modulus of elasticity of fiberglass posts is the most similar to the modulus of elasticity of dentin, giving strength and longevity to the restoration of endodontically treated teeth, information that is presented in Table 1. However, the present work will not study the use of fiberglass, but titanium.

Unlike natural teeth, when applying non-axial forces to an implant, it will perform a secondary movement that varies between 10 to 50 $\mu$m, this mobility is associated with bone viscoelasticity and does not cause a rotation towards the apex as it happens in a natural root, resulting in the concentration of forces in the bone crest [11].

Analogously to Figure 2.2, Figure 2.4 performs the finite element analysis, but in five different types of dental implants. It can be observed that, regardless of the model, the stresses tend to be concentrated in the bone crest, an analysis that was also completed for natural teeth.

Table 2.1: Elasticity modulus of dental materials compared to dentin, adapted from [20][21].

| Material | Elasticity Modules [GPa] |
|----------|--------------------------|
| Composite Resin | 15 |
| Fiberglass | 40 |
| Titanium (CP) | 90-100 |
| Ceramics | 170 |
| Dentin | 18.3 |
| Carbon Fiber | 66-130 |
| Grade 5 Titanium | 114 |
| Cortical Bone | 11-20 |
| Medullary Bone | 1.3 |
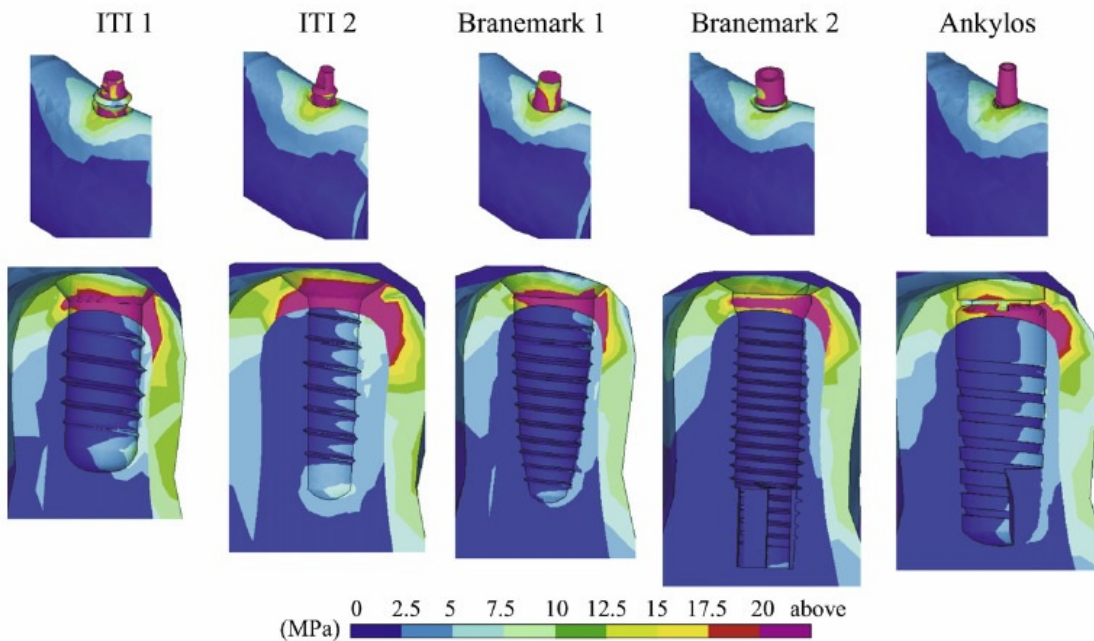


Figure 2.4: Finite element analysis in mandibular implants [12].

The main benefit of a fixed prosthesis over a mobile one is the non-movement of the position in the mouth during daily activities, such as eating and speaking. Thus providing

well-being to the patient.

For the implants to function properly, the biomechanical characteristics are extremely important, since, if the body rejects the implant, it will not be able to perform its functions correctly, causing its removal. Occlusal overloads can also have consequences, such as the initial loss of the bone crest and the generation of implant micromovements [19].

In Figure 2.5 it is possible to visualize the comparison of the structure of a natural tooth and a dental implant.
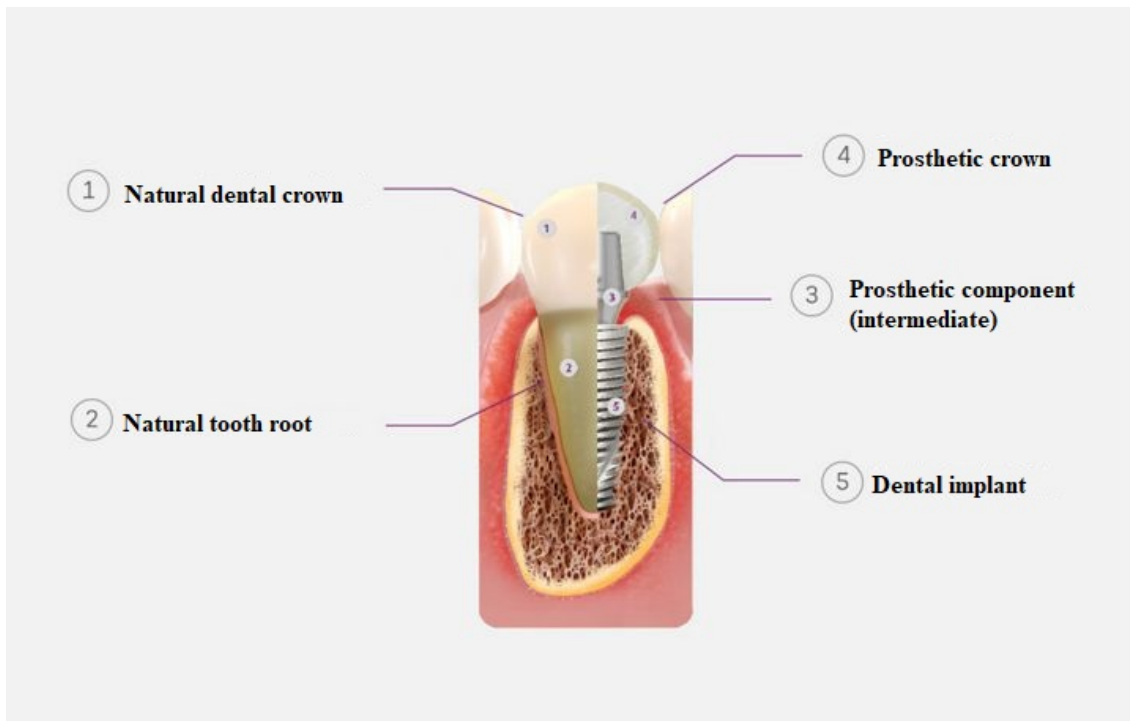


Figure 2.5: Comparison of the structure of a natural tooth with a prosthesis over the implant [22].

### 2.3.1 Types of Implants

As seen in Figure 2.4, there is a variety of dental implants, each with its own specifications, for each case of patient need.

One of the factors for choosing the implant is the fixation site and what type of bone will be implanted. Misch described a classification for four bone types, and the one most

found in implant dentistry is found in the literature as shown in Table 2.2 [23].

Each bone type is found in specific areas. For implant dentistry, good primary stability is necessary, where it is acquired in its insertion into the bone, during surgery, it also needs sufficient blood irrigation so that the local metabolism is not harmed and facilitates healing, and consequently, osseointegration [24].

Table 2.2: Bone types and their characteristics for implant placement, adapted from [24].

| Bone Type | Description | Good Primary Stability | Good Blood Irrigation | Comments |
|---|---|---|---|---|
| I | Dense cortical | Yes | No | Not good candidate for implant placement |
| II | Dense cortical and thick trabeculate | Yes | Yes | Ideal for implantation of prostheses |
| III | Thin cortical bone and fine trabecular bone | Medium | Medium | More stable than type IV bone |
| IV | Thin trabecular meshwork | No | Yes | No good candidate for implant placement |

Therefore, for a good osseointegration, the ideal would be the implantation of type II bone implants; however, this bone is commonly found only in the mandibular anterior region when not very resorbed. [24]

Table 2.4 describes some general information about Neodent implants for comparison purposes between two implants of the Titamax EX CM line, the Titamax Ti EX and the Titamax Ti.

Table 2.3: Comparison between the types of implants of the neodent brand of the Titamax EX CM line [18].

| | Titamax Ti EX | Titamax Ti |
|---|---|---|
| General information | Cylindrical body and double threads for minimal trauma and faster installation. High compaction power (bone expansion), external hexagon interface | Cylindrical body and double threads, high cutting power and external hexagon interface. |
| Recommendation | Type III and IV bones and areas of thin bone due to subinstrumentation | Type I and II bones and bone graft areas en bloc. Upper and lower lateral incisors. |
| Drilling speed (rpm) | 500-800 | 800-1200 |
| Insertion speed (rpm) | 30 | 30 |
| Maximum torque (N.cm) | 60 | 60 |

14

Table 2.4: Comparison between the types of implants of the neodent brand of the Titamax EX CM line[18].

| | Titamax Ti EX | Titamax Ti |
|---|---|---|
| General information | Cylindrical body and double threads for minimal trauma and faster installation. High compaction power (bone expansion), external hexagon interface faster installation. High compaction power (bone expansion), external hexagon interface | Cylindrical body and double threads, high cutting power and external hexagon interface. |
| Recommendation | Type III and IV bones and areas of thin bone due to subinstrumentation graft areas en bloc. Upper and lower lateral incisors. | Type I and II bones and bone |
| Drilling speed (rpm) | 500-800 | 800-1200 |
| Insertion speed (rpm) | 30 | 30 |
| Maximum torque (N.cm) | 60 | 60 |

## 2.3.2 Materials applied to dental implants

Restorative dental procedures aim to preserve the dental structure. With the evolution and further development of restorative materials, enhancement, quality, agility, and aesthetics have been considered important. And consequently, it has provided more options for re-establishing the patient's masticatory appearance and function [25][26].

Quality seeks components with physical and chemical properties close to dental structures, thus allowing good clinical behavior. Agility, on the other hand, seeks to reduce clinical time, maintaining or improving process performance.

The main material used for dental implants is titanium, and in this chapter, its characteristics and reasons for using it will be explained.

**Titanium**

Titanium is a lightweight, high-strength metal that is solid at room temperature. It is not a good thermal conductor, but it has a high electrical conductivity. In its pure state, this metal is ductile and therefore easy to work with. Titanium's biggest advantage is that it is as strong as steel but 45% lighter [27].

Due to its lightness, it is widely used in alloys for application in the aeronautical and aerospace industries, and it also has the advantage of withstanding high temperatures, which is ideal for missiles and spacecraft. The use of Titanium in dental implants and

bone prostheses is explained by the lightness of the material and the biocompatibility that guarantees patient comfort. In Figure 2.6, it is possible to visualize the application of titanium in a biomechanical environment.



Figure 2.6: Example of a titanium implant [28].

Titanium has general properties that promote its use as a biomechanical material, with high corrosion resistance and excellent biocompatibility/osseointegration being the main ones, in addition to low density and low thermal conductivity. The latter is important because it allows the patient to eat food at different temperatures without suffering any type of thermal shock [29][30][31].

But it also has some negative characteristics, such as the high cost of handling equipment; elaborate casting techniques, since titanium is highly reactive when liquid to the atmosphere, therefore it must be controlled throughout the process, it is not possible to use conventional welding methods, only laser; high melting point (1688ºC) which has the particularity of a marked difference in temperatures between the mold and the metal, making it difficult to solidify and enabling porosity, incomplete castings or internal stresses [32][31][29].

Like steel or aluminum, titanium has several alloys such as CP (Commercially Pure), grade 3 (Ti 3Al-2.4V, Ti 3Al-8V-4Mo-4Zr, and the like), grade 4 (Ti 6Al-Nb, Ti 6Al-4V and the like), and several others. CP alloys are classified into 4 types and have different characteristics between the models of corrosion resistance, ductility, and mechanical strength. For example, the first category of CP alloy has greater corrosion resistance, good ductility, and lower strength, while the fourth has worse corrosion resistance, moderate ductility, and better strength [33].

The purer the titanium is, the less mechanical strength it has, however, greater resistance to oxidation. Despite the variations in the chemical composition of each type, their physical properties do not appear to change significantly. The most common Titanium alloy for implants and medical devices is grade 5, Ti 6Al-4V, which has improved mechanical properties and toughness. It is observed that this grade 5 alloy has more elements than CP and will reflect on its mechanical strength. Some useful data from this particular Ti are shown in Table 2.5 below [33].

Table 2.5: Mechanical Properties of a Grade 5 Ti 6Al-4V [21].

| Mechanical Properties | Values | Unit of Measurement |
|---|---|---|
| Yield Tensile Strength | 1100 | MPa |
| Ultimate Tensile Strength | 1170 | MPa |
| Modulus of Elasticity | 114 | GPa |
| Poisson's Ratio | 0.33 | |

For the comparisons carried out in this work, the Ti 6Al-4V alloy will be used due to its wide use in biomechanics. To increase the accuracy of the simulation, the Ti was considered a bilinear material, using the Bilinear Isotropic Hardening function inside Engineering Data with the values of the table above.

### 2.3.3 Preload

The force that keeps the implant components connected is called preload and is described as an axial tension along the screw. The torque exerted on top of the retaining screw has the unit of measurement Newton centimeter (N.cm), commonly used in dentistry. The moment applied by torque is responsible for the union of the internal and external threads of the implant body [34][35][36].

To perform the preload, manufacturers indicate 32 N.cm for titanium screws. The preload created on the screw thereafter must be between 60% and 75% of the yield limit of titanium [37][38].

By not reaching the intended preload, there is a decrease in the system's survival, they may lose screw retention, which results in connection separation. Thus, when excessive torque is applied, they can cause failures by deforming their threads [39].

The non-axial forces applied to the implant, generate moments of forces proportional to the distance from the axis of the implant, see Figure 2.7 [40].
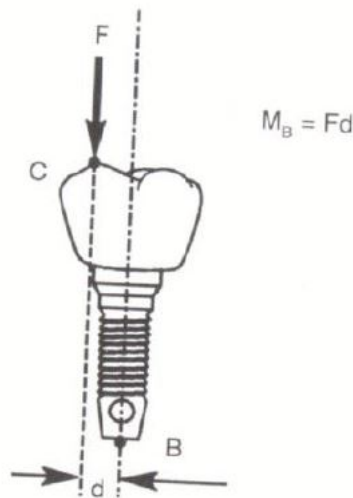


Figure 2.7: Non-axial forces applied to the prosthesis [40].

For comparison purposes, the retaining screw can be compared to a spring, which is stretched by the preload and maintains the stretch of the threads through frictional forces.

18

The indicated preload value, as already mentioned, is between 60% and 75% of the yield limit of titanium, given by the modulus of elasticity in the stress/strain diagram. The plastic transformation phase, in which the deformations are permanent, starts as soon as the stress exceeds the proportionality limit. These deformations cause the screw to loosen, and if the stresses exceed the material's strength limit, the entire system fails [38][36].

It is extremely important that the dental surgeon understands the biomechanics of bolted joints, as this increases the probability of reaching the ideal preload. In addition to mechanical complications, failure of connections can also end up generating biological problems, such as bone loss, compromised osseointegration, and soft tissue sequelae, including sensitivity, inflammation, and gingival hyperplasia, which is the increase in the number of cells in the gums, causing a small swelling of the gum between the teeth [36][41].

An osseointegrated installation in the form of a screw can transmit tension load or axial compression to the bone that surrounds the implant, a screw will not suffer initial or internal tension if, during its healing, there are no loads on it [42].

The mechanical stress that is transferred from the implant to the bone must be taken into account, as neither the implant nor the bone should be stressed beyond the capacity of long-term fatigue. Furthermore, it is important to ensure that there will be no relative movement that produces bone abrasion or progressive loosening of the implant [43].

The consequences of failures in the implant/crown union can impair the good performance of the implant, produce unforeseen efforts and result in severe damage to both the bone and the implant itself, fail in rehabilitations, exceed the physiological limit, and cause loss of osseointegration [44].

### 2.3.4   Osseointegration

In 1981, Branemark defined from a magnification, with the aid of an optical microscope, that osseointegration dealt with the direct contact between the living bone and the surface of an implant, which, the material commonly used due to its compatibility was titanium and its alloys. Thus, it is expected that if there is an overload of any kind to the system,

the failure will occur firstly on the part of the bone and later on by the implant itself. In Figure 2.8, it is possible to visualize the representation of an implanted titanium pin and, consequently, the osseointegration [19].



Figure 2.8: Implanted titanium pin [45].

Osseointegration is the first phase of implant healing, and also the main one affected by its surface condition. That is, the success of osseointegration, which is complete healing, is directly linked to the conditions of the implant surface [19].

Before studies on the importance of osseointegration, implant-supported prostheses tended to move and consequently fail, and even implant loss could occur. This happened because there was the formation of a fibrous structure around it.

The success of long-term osseointegrated implants depends on the following factors: quality and quantity of bone tissue in which they are anchored, quality of materials used in their manufacture, adequate surgical and prosthetic techniques, and also on the choice of infrastructure and prosthetic components, which enables the distribution of masticatory and parafunctional loads in each implant, individually [44].

20

## 2.3.5 Loading Conditions

The load that a tooth can support depends on several factors, including some related to food, such as type, quantity, texture, and stiffness. Consequently, studying all hypotheses makes the work unfeasible. To solve this problem, the loading parameters will be based on and similar to those presented by Gomes and O'mahony. A force of 133 N is then presented at an angle of 30° from the vertical and applied at 2 mm displaced along the axis of the implant [12][46].

For interpretation purposes, the Figure 2.9 show the previous explanation about the loads on the crowns.
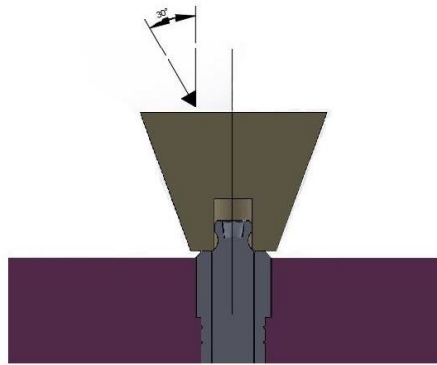
Figure 2.9: Force at 30° and 2 mm displaced along the axis.

## 2.3.6 Friction

The only form of friction considered in this work is between the titanium faces (Ti-Ti). The other contacts were considered bonded as there is little movement between the parts. Friction is represented by the following formula:

$$F_{sf} = \mu_s . N \tag{2.1}$$

Where, $F_{sf}$ is the static friction force and $\mu_s$ is the static friction coefficient.

The friction between the titanium is considered static because the implant is already correctly assembled and the simulation is static, that is, there are no dynamic conditions.

The Static Friction ($\mu_s$) considered to this project is 0.34 [47].

## 2.4 Polymers

The word polymer is derived from the classical Greek words poli, meaning "many" and meres, meaning "parts". A polymer is a long-chain molecule composed of a large number of repeating units of identical structure. Nowadays, polymeric materials are used in almost every area of everyday life and their production and manufacture is in major industries around the world.

The classification and definition of polymers, silicones and hyperelastic as a single set of compounds are very broad and is beyond the scope of the present work. In this review, we will focus on Polydimethylsiloxane (PDMS) used as precursors in the synthesis of protective films. This polymer can be classified as a hyperelastic material, which is characterized by large deformations [48][49][50].

### 2.4.1 Polydimethylsiloxane (PDMS)

Polymers are formed through the chemical bonding of smaller molecules, called monomers, in addition, depending on the number and characteristics of these molecules, different properties can be obtained [51].

Polydimethylsiloxane (PDMS) is the most used silicone based on organic polymers and presents the characteristics of a transparent and flexible compound with biocompatibility properties. As can be seen in 2.10, it has silicon and oxygen bonds in its chain [52]. PDMS has low temperature properties at which it can cure and is about 50 times cheaper than monocrystalline silicon. Furthermore, its reversible deformation capability makes it favorable in single-membrane actuators [53].

There are several manufacturers of this product on the market, but PDMS Sylgard ® 184 was chosen to do this job. The material is supplied in two components, the prepolymer and the curing agent, which will be mixed according to a specification ratio that depends on the desired characteristics of the final product.

22

PDMS is used in the biomedical area; thus, the material has high biocompatibility and biostability. This means that the use of the material does not cause adverse effects when in contact with biological tissues [54]. This is because the biocompatible material and biomechanical behavior are similar to biological tissues, with applications in the study of aneurysm behavior and devices such as micropumps and optical systems [55][56].

The incompatibility of mechanical properties can cause inflammation or support to present stresses, this is related to structural biocompatibility, mechanical interactions between an implanted device and the surrounding tissues environment [55].

The main advantages of PDMS are: easy fabrication, non-toxicity, non-flammability, optical transparency [57], biocompatibility [58], high compressibility [59], high flexibility [60], viscoelasticity, and is chemically and thermally stable [61]. In addition, PDMS is capable of modifying and blending with other materials, further expanding its application range [62].
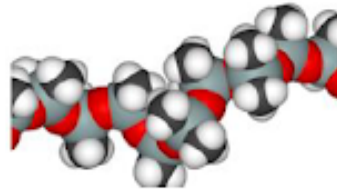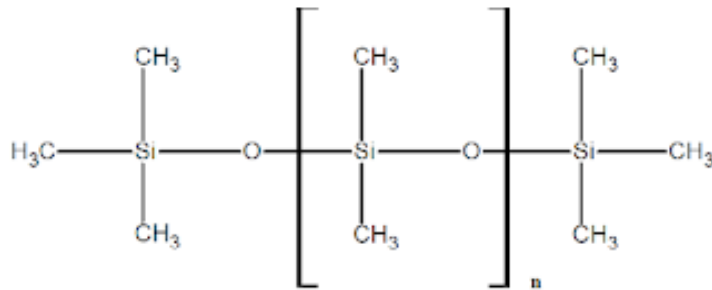


Figure 2.10: Chemical structure of PDMS [63].

PDMS also offers high elasticity values [64] due to the fact that it exists in a very compact form. Thus, when subjected to a tensile force, the polymer is stretched, and returns to its initial state when the load is interrupted, releasing its tension.

**Chemical and Mechanical Properties of PDMS**

Considered inert, thermally stable, permeable to gases and easily handled at room temperature, PDMS is a material with isotropic and homogeneous properties, as well as reduced costs and is an ideal material for the development of microstructures [65].

PDMS, when applied to arterial prostheses, is under constant blood pressure effect, so in these cases it is extremely important to know the characteristics of the material so that the force to which it is subjected does not lead to rupture. The mechanical behavior of a material represents its response when subjected to a load or force being exerted [66].

Experimentally, the mechanical properties of materials are obtained by carrying out tensile tests that reproduce the loads to which they can be subjected on a daily basis. The intensity of the load to be applied, the time that will be subject to this load and the speed of application must be taken into account. This load can be tensile, compressive or shear, and its magnitude can be constant over time or vary continuously [66].

**Chemical Curing of PDMS**

PDMS is supplied in a kit consisting of two chemical products in a liquid state, one of which is the base and the other the hardener. After the occurrence of mixing these two components, it is verified that the PDMS in the liquid state becomes rubber. The ratio recommended and adopted by the manufacturer Sylgard® is 10:1, with the base being the greater part and the hardener being the smaller proportion.

## 2.5   Engineering Curve

When the distribution of stresses in a cross-sectional area is considered uniform, this stress ($\sigma$) is given by dividing a tensile force F applied at each point over the initial cross-sectional area $A_0$. The SI unit for this quantity is Newton per square meter [N/m2] or Pascal [P] (Equation 2.2) [67].

$$\sigma = \frac{F}{A_0} \tag{2.2}$$

When the uniaxial tensile force acts on the specimen, it causes a deformation ($\varepsilon$) which is given by the ratio between the variation of length (l) and initial length ($l_0$), being translated by Equation 2.3.

$$\varepsilon = \frac{l - l_0}{l_0} = \frac{\Delta}{l_0} \tag{2.3}$$

In Equation 2.4 it is possible to verify the linear deformation of a structure, which deforms due to the magnitude of the stress imposed on it. Equation 2.4 refers to Hooke's law, where the proportionality constant E is the modulus of elasticity [66].

$$\sigma = E.\varepsilon \tag{2.4}$$

The deformation process in which stress and deformation are proportional to each other is called elastic deformation, and its graphic representation is a straight line as shown in Figure 2.11.
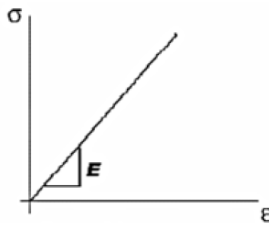


Figure 2.11: Hook's Law [67].

However, this law is not valid for all strain values, it is only an approximation when the stress is relatively low, taking into account the type of material to be evaluated. Elastic deformation is not permanent, so when the load is no longer applied, the piece returns to its original shape [66].

Young's modulus (or modulus of elasticity (E)), can be defined as the variation in

strain as a function of stress. As a rule, this mechanical property can be obtained through the slope of the straight line in a stress-strain diagram. The tangent of the modulus of elasticity is the slope of the diagram referred to (Figure 2.12) at any point, on the other hand, the secant of Young's modulus is the ratio between stress and strain for any stress or strain value [68].
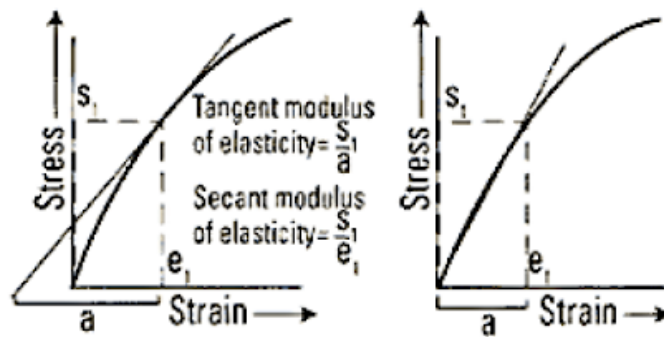


Figure 2.12: Stress-Strain Diagram [68].

Tensile testing is one of the most used procedures to assess various mechanical properties of materials such as modulus of elasticity, yield strength, rupture strength, and deformation Which will be used in the project [67].

This consists of using a specimen of a certain material with a standardized shape and dimensions which is subjected to a uniaxial traction force that will stretch or elongate it until its rupture occurs. The load and tension exerted will gradually increase and is applied uniaxially along the longest axis of the specimen, which may be circular or rectangular.

As a rule, during the test, the deformation occurs essentially in the central region of the specimen since this is the region with the smallest transversal area. In turn, the test piece is held by the machine's ties that pull it at a constant speed defined at the beginning of the test, and the load and the elongation resulting from the tensile test are measured. This type of test is called a destructive test because in the end the specimen is destroyed [66].

In the tensile test, the force and elongation are registered, which allows calculating the stress (Equation 2.3) and the deformation (Equation 2.4), giving the engineering curve, as shown in Figure 2.13.
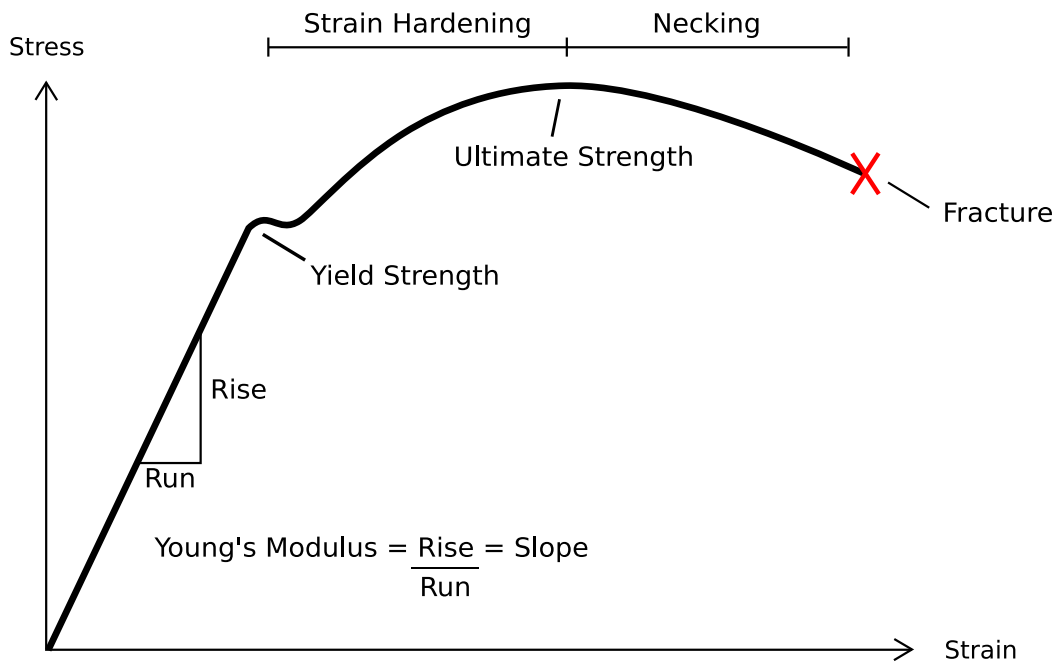
Figure 2.13: Stress-Strain Diagram, adapted from [69].

The real Stress-Strain graphic is very complicated. In some applications, a simplification may occur. A very simple simplification is the linear approximation, it only displays the elastic behavior of the element, and after that point has passed, this method turns to be inaccurate. The bilinear approximation otherwise, has the capability of the elastic behavior and the plastic behavior as well until the Ultimate Tensile Strength. Finally, the multilinear one has an equation for every step along with the graphic, however, it is hard to have it unless the author did some tests on the material.

27

## 2.6    Mesh Convergence

The accuracy and success in determining a slope meshing will depend on how the FEM parameters such as mesh size, element shape, number of elements etcetera, are selected. A fine mesh can be specific; however, it is computationally costly [70].

It is necessary finding a good mesh that is not too rough, it would not give accurate results, or not too fine, it would have a high computational cost. Consequently, it is needed to know how to find this balanced mesh.
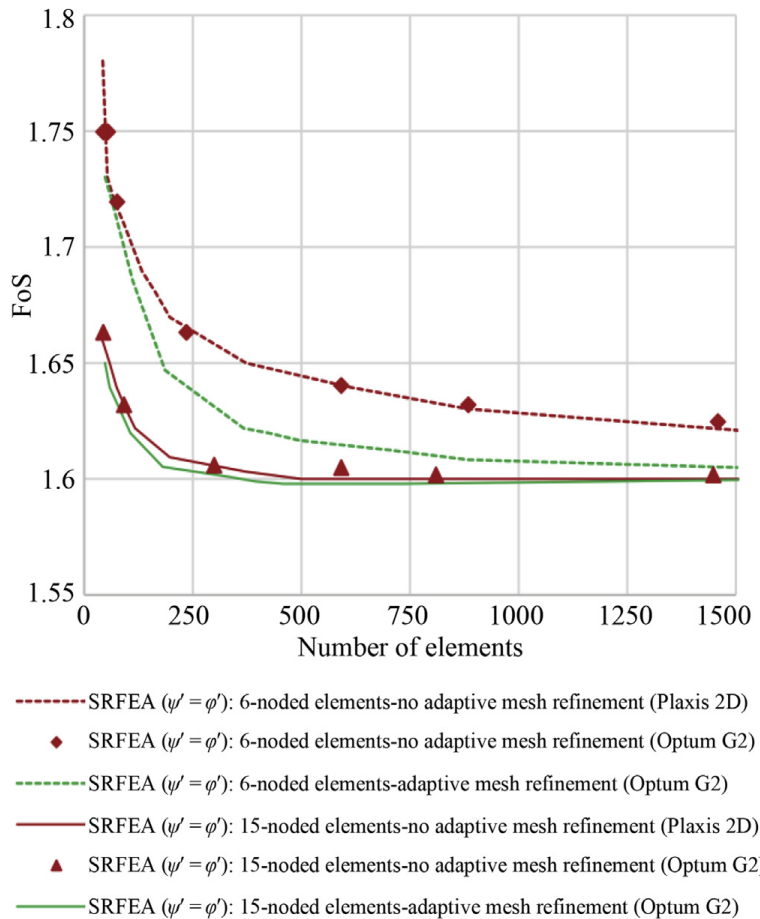


Figure 2.14: Factors of safety obtained from SRFEA (Strength Reduction Finite Element Analysis) with different numbers of elements, adapted from [71].

A nice mesh could be discovered by doing analysis just like shown in Figure 2.14. After the increase of meshing, the value did not change much, and the tendency is that

the graphic shows it will not change anymore. Consequently, the optimal point should be near 500 elements for a 15 node elements, or 1500 elements for a 6 node elements for this specific analysis [72].

The same logic should be valid in this project. This means that it is necessary to find the mesh convergence of this geometry by pilot simulation and then work near that point applying the same characteristics for the full model that will be studied. The implant can be simplified to 1/2 of the original just to find the balance point, and then extrapolate it to the entire geometry.

# Chapter 3

# Methodology

This chapter describes all laboratory and computational activities performed in this dissertation. The Fuid Mechanics and Hydraulic Laboratory (LMFH) of the Polytechnic Institute of Bragança (IPB), was used to carry out the laboratory procedures. The Virtual Machine of the IPB was used to do the simulations.

## 3.1 Mold Production

The mold was previously manufactured according to the ASTM D412-16 standard. In Figure 3.1, below, it is possible to observe its real photo.

In Figure C1, located in Appendix C, the geometry and dimensions of the specimen was represented in a Technical Drawing, following the references of the ASTM D412-16 standard.

Figure 3.1: Picture of used mold.

Four aluminum alloy molds (Al 2011-T3) were used, machined in a computerized numerical control (CNC) machine, Deckel Maho DMC 63V. The molds were cleaned, sterilized, and dried. It was estimated that the mass of each specimen would be 7g, being four specimens, 28g of PDMS were made with space for error.

## 3.2   Production of the specimen

Slygard 184 brand PDMS is in a liquid state, so for its manufacture, a manual mixture of a prepolymer in a proportion of 1:10 was made, using 25.51 g of base and 2.54 g of hardener. The weighings were performed on a digital scale and are shown in Figure 3.2.
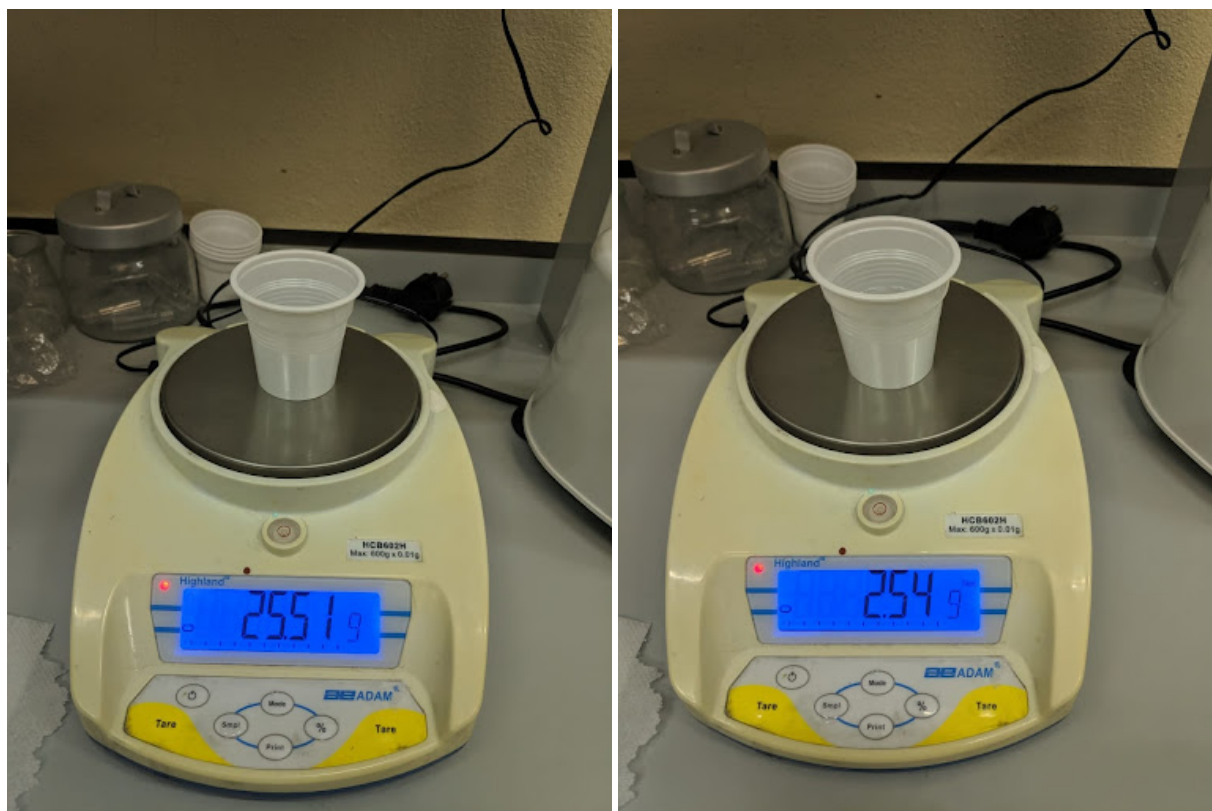
Figure 3.2: Weight of the prepolymer and hardner.

After mixing the two components, the PDMS was stirred for about 5 minutes with the aid of a spatula in a clockwise direction. After this, the container containing the PDMS was placed in the desiccator connected to the vacuum pump, Figure 3.3, thus removing most of the bubbles from the mixture. This process took about 5 minutes. These bubbles could, at a later stage, alter or compromise the results of the experiment.

When the mixture was homogeneous and without the presence of bubbles, it was poured by gravity into the molds. After that, it was taken back to the desiccator to remove the rest of the bubbles present. After this, the PDMS was cured for 48 hours at room temperature, to cure slowly, leading to the release of possible existing bubbles. After that, it stayed untouched for another 7 days to be able to carry out the tests.
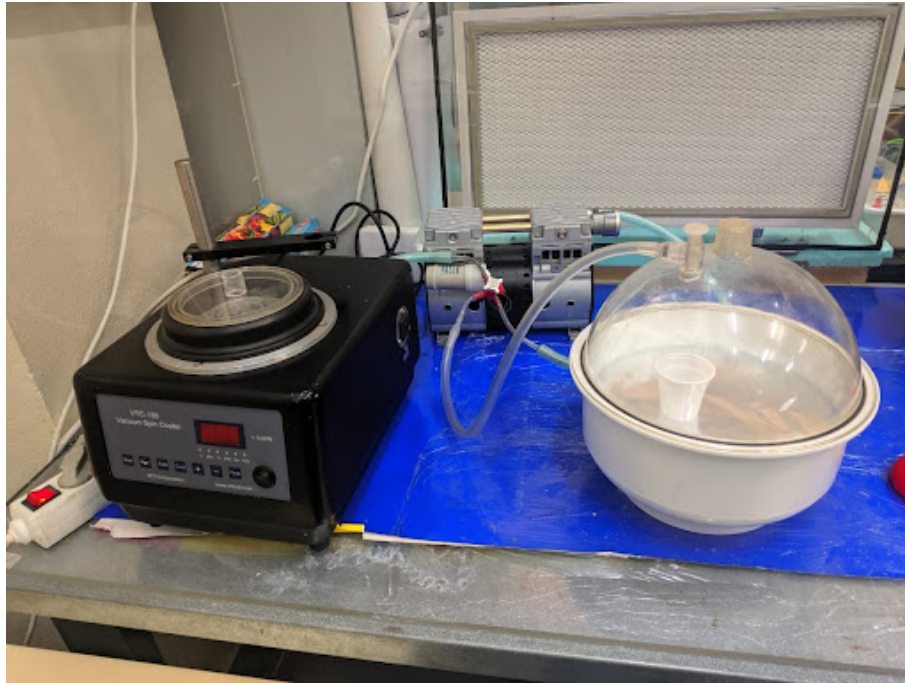
Figure 3.3: Vacuum chamber used.

For the PDMS drying/maturing process, steel support was on a level table horizontally and vertically for better uniformity, shown in Figure 3.4. After these steps, the specimen was ready for tensile tests.
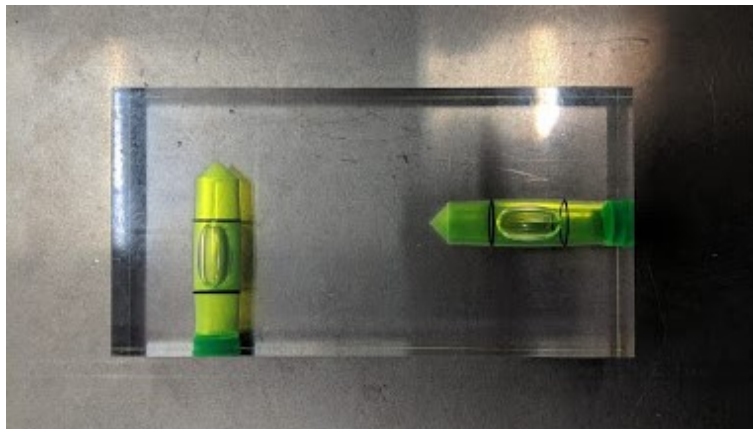


Figure 3.4: Steel support for leveling.

## 3.3 Tensile Test

On the universal testing machine, Shimadzu ® Autograph AGS-X 10KN, its claws were positioned 70 mm apart, the strain gauges in the center with a 20 mm opening, thus it was possible to start the tensile test. The test speed was set to $500 \pm 50$ mm/minute according to the D412-16 standard. In Figure 3.5, the tensile test is represented.
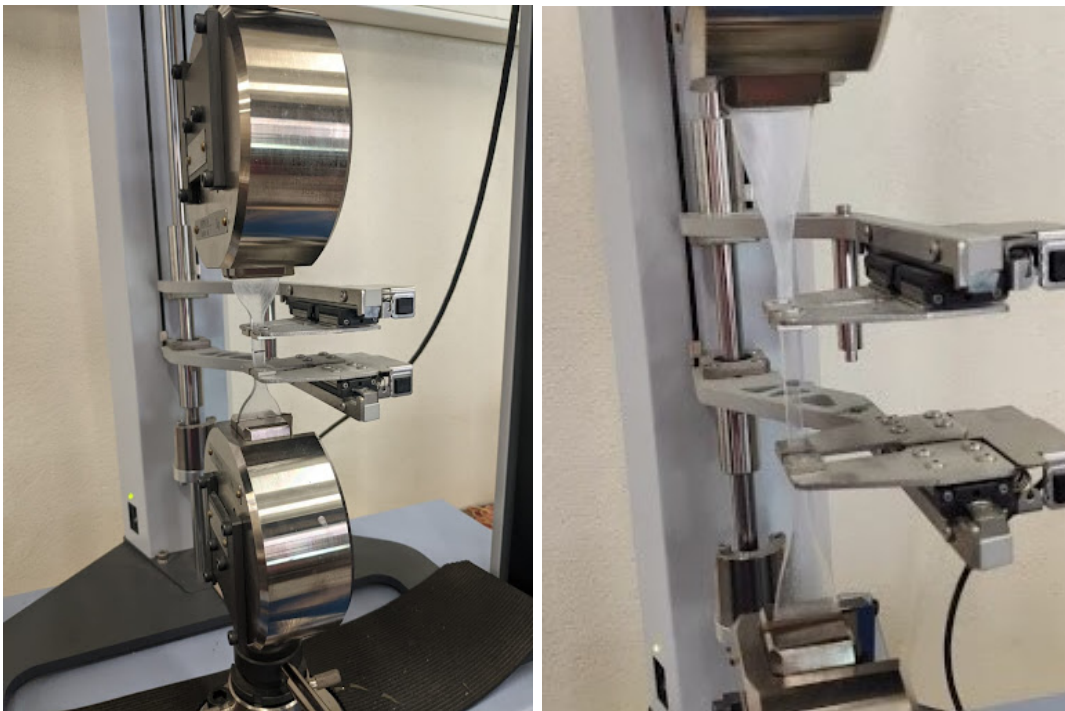


Figure 3.5: Picture of the tensile test in the specimen.

After performing the tensile tests, the universal machine controller software provides the necessary data through tables. The time corresponding to each applied force generating a displacement.

The time for this work is not relevant, as the interesting thing here will be to evaluate the stress and strain, so it was necessary to work on the spare data.

To get the stress values, simply divide the instantaneous force applied by the cross-sectional area of the specimen. As for the strain, it is necessary to use the displacement, which is the instantaneous length minus the initial length and divide it by the initial

length itself, so we will have a dimensionless value.

One new material was then created in the Engineering Data tool within the Ansys Workbench with the data taken from the tests already carried out. Some basic simulations were performed in order to validate the collected data.

## 3.4   Implant Modeling



Figure 3.6: Photo of the real implant in enlarged scale (5:1).

The implant is a five times magnified scale of the actual implant, like is shown in Figure 3.6. Measures were taken with the aid of a pachymeter, micrometer, and an image projector in the UTFPR-CP Metrology Laboratory, shown in Figure 3.7. With the increased scale measurements, it was possible to draw the real implant in Solidworks. Figure 3.8 shows the three parts exactly as they should be.
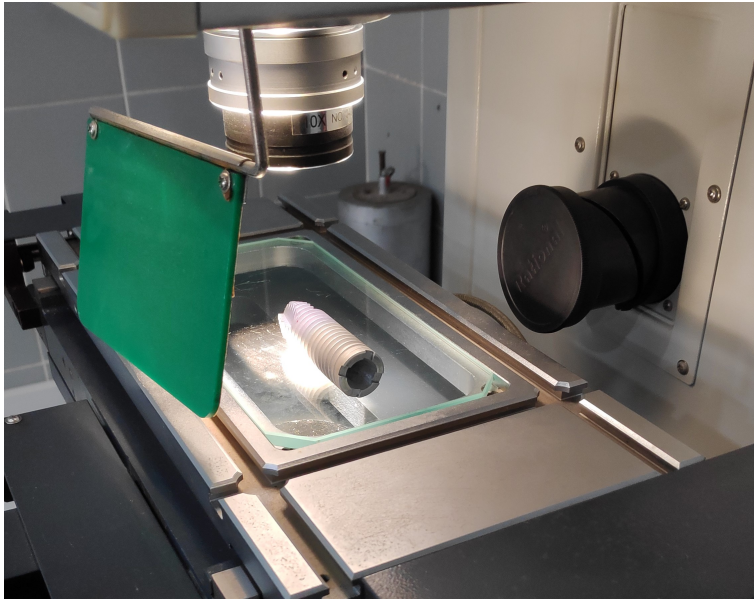
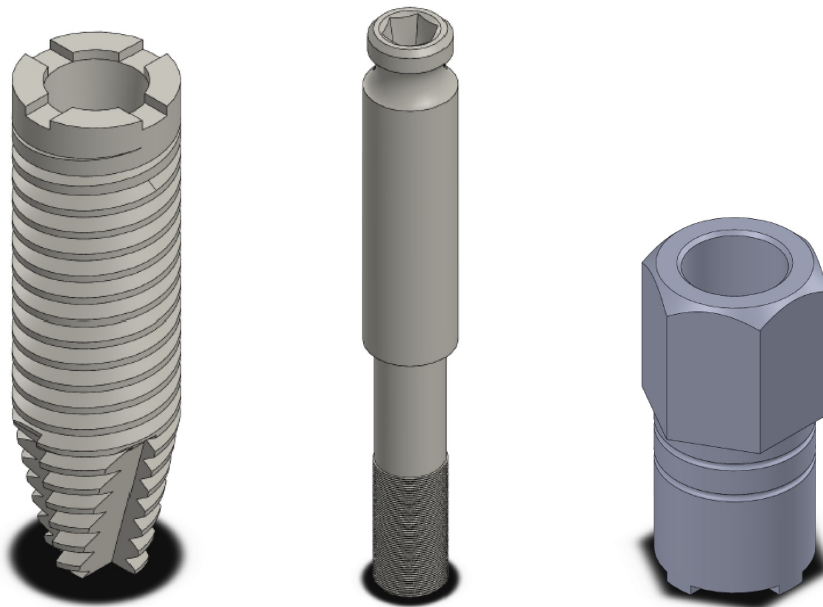Figure 3.7: Picture of dimension acquisision aided with a image projector.



Figure 3.8: Picture of the implants parts in a 3D CAD software.

The computer that will be used to carry out the simulations has processing limitations, so each feature that is simplified will reduce significantly the processing time. The study

that will be carried out is a static analysis, the relative movement between the threads is very small, or even null. It will be simplified for smooth and bonded surfaces. The rest of the contacts will be considered as frictional. Another features were disregards, for example the cut in the bottom of the screw, the groove on the crown and on the pillar, etcetera.

## 3.5   Numerical Simulations

In the Ansys Workbench, three simulations were performed as "Static Structural Analysis", the first with only the specimen, the second with the implant without a film, and the third with the implant with a 0.2mm PDMS film.

### 3.5.1   Specimen

For the first simulation, the geometry of the specimen was imported in "geometry". The 3D drawing was simplified into a 2D in the "Design Modeler" to decrease the graphic cost.

As the simulation use PDMS material, it was necessary to create a new material in the software in "engineering data", with the data taken from the experimental tests. The material was given the name PDMS.

It was also necessary to add the "linear elastic" feature and import the "uniaxial test data" into the "hyperelastic data" to the new material. The temperature at which the test was performed, 25°C, was also added, but in this case, it makes no difference since there will be no thermal analysis.

The data table from the tensile tests (Strain [m/m] by Stress [MPa]) was imported and the Mooney-Rivilin 5 Parameters hyperelastic resolution method was added. This model provide the best accuracy for nonlinear materials with Strain range between 30 and 200%, which covers most of the PDMS strain and better than any other method work [73]. Explaining and applying all of the hyperelastic solving models are beyond the scope of this work, since are several methods, it would be very extensive and complicated.

The equations were solved by "Curve Fitting Solve Curve Fit", the results were copied in "Copy Calculated Values To Property" and paste the values in the constants.

In "mechanical" the object geometry was designated by "PDMS", the object mesh was created with sufficient refinement not to interfere in the results.

The lower edge of the object was considered as "fixed support" and on the upper edge there is an increasing force from 0 to 100N upwards. See Figure 3.9.

Based on the physical test, the lower flap was considered as fixed support, as the grip of the tensile testing machine does not move, and the upper flap is pulled with a force of 100N. The meshing method used was Tetrahedrons.
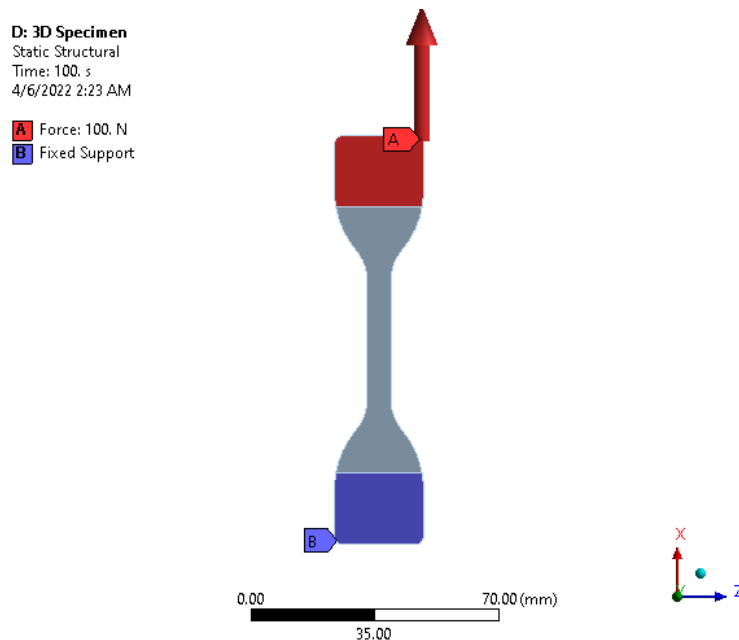


Figure 3.9: Boundaries conditions of the specimen in the tensile test.

The desired studies were added, in this case, the "Equivalent Elastic Strain (von-Mises)", "Equivalent Stress (von-Mises)", and "Total Deformation" to study the problem. With the results, it is already possible to analyze whether the results are compatible with those of the physical test with some arbitrary values.

### 3.5.2 Implant

For the simulations of the implants, the procedure is the same, the only differences are the addition of Titanium Grade 5 and Medullary Bone in the Engineering Data, making the connections, friction and bonded, between the items according to the real implant, the fixed support, and the force, which is applied in other areas.

As explained before, this project will consider the Ti 6Al-4V as a bilinear material with 1100 MPa of Yield Tensile Strenght and 1170 MPa of Ultimate Tensile Strenght. The Medullary Bone is considered simpler, only a linear material.

Regarding the connections between the parts, pillar, crown, bone, base, and PDMS film, which are threads, they were assumed to be bonded, as there is no relevant movement. All others were considered to have the friction of 0.34, value to Ti-Ti [47].

All of the connections are illustrated in Appendix A. For the implant without film, the connection were shown in Figures A.1(Bonded), A.2(Bonded), A.3(Bonded), and A.4(Frictional). Similarly, for the implant with film, Figures A.6(Bonded), A.5(Bonded), A.2(Bonded), A.3(Bonded), and A.4(Frictional).

The Figure 3.10 shows the boundaries conditions of the implants. It represents both cases that will be simulated, without film, and with 0.2 mm film. The force is aplied in the xy plane, angled and dislocated as specified in the Theoretical Foundations.

For the simulation to be accurate, the option Large Deflection, inside Analysis Setting, should be on, since the PDMS is a hyperelastic material and, consequently will have large deformation. For the solver to manage the simulation correctly, the force applied should grow gradually, otherwise, the criterion would hardly converge. It was chosen to have 133 steps or 133 seconds, the same value as the force applies (133 N in modulus, explicit in Theoretical Foundations, Section 2.3.5), this way, each step will have 1N/step or 1N/1sec in this case. Further, The Minimum Time Step was set to $10^{-6}s$ and the Maximum to 1s, in other words, the minimum step was set to $10^{-6}N$ and the maximum to 1N. Ansys recommended using a Newton Raphson Method as Asymmetric because of the high friction values to help it converge. The meshing method used was Tetrahedrons.
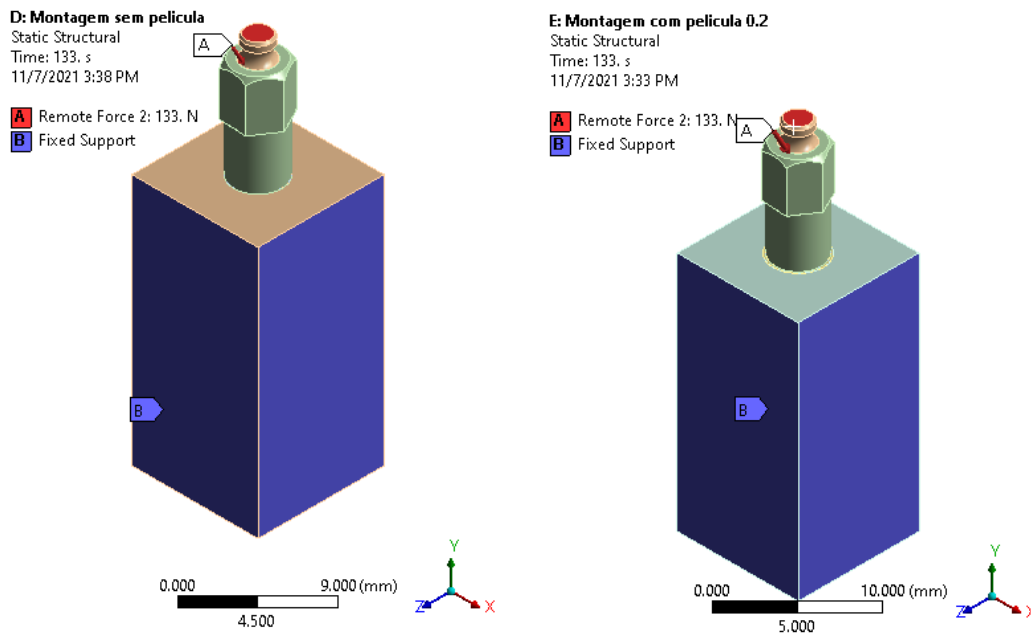
Figure 3.10: Boundaries conditions of the implant in the simulations, without film on the left, and with 0.2 film on the right.

The meshing of the model is a more complicated process. First, it's needed to know where the critical areas are, then discover how fine the mesh needs to be. Based on that, some implant simulations with standard and then finer customized mesh were done. The critical areas discovered are shown in Figure 3.11. The logical procedure is to refine only the sufficient for each body and face. The critical faces, however, requires much finer mesh, to find out how fine it should be, new simulations only changing the critical variables were made.

Table 3.1 shows the mesh sizing for each case in mm, the "B." represents the body sizing, and the "F." the face sizing. As the case changes, the mesh size in the critical regions is reduced by 25%, for example, the value of the face sizing of case 2 is 3/4 of case 1, and so on. The 1/F means the calculus made of the face sizing of crown or pillar, since they are the same, it is used to make a graphic shown in the next chapter.

Table 3.1: Meshing Sizing: simulations of 1/2 of the implant without film [mm].

| Name | B.Screw | B.Bone | B.Pillar | B.Crown | B.Bone | F.Screw | F.Crown | F.Pillar | 1/F |
|------|---------|--------|----------|---------|--------|---------|---------|----------|------|
| 1 | 0,75 | 1 | 0,3 | 0,3 | 0,5 | 0,5 | 0,5000 | 0,5000 | 2,0000 |
| 2 | 0,75 | 1 | 0,3 | 0,3 | 0,5 | 0,5 | 0,3750 | 0,3750 | 2,6667 |
| 3 | 0,75 | 1 | 0,3 | 0,3 | 0,5 | 0,5 | 0,2813 | 0,2813 | 3,5556 |
| 4 | 0,75 | 1 | 0,3 | 0,3 | 0,5 | 0,5 | 0,2109 | 0,2109 | 4,7407 |
| 5 | 0,75 | 1 | 0,3 | 0,3 | 0,5 | 0,5 | 0,1582 | 0,1582 | 6,3210 |
| 6 | 0,75 | 1 | 0,3 | 0,3 | 0,5 | 0,5 | 0,1187 | 0,1187 | 8,4280 |
| 7 | 0,75 | 1 | 0,3 | 0,3 | 0,5 | 0,5 | 0,0890 | 0,0890 | 11,2373 |
| 8 | 0,75 | 1 | 0,3 | 0,3 | 0,3 | 0,3 | 0,0667 | 0,0667 | 14,9831 |
| 9 | 0,75 | 1 | 0,3 | 0,3 | 0,3 | 0,3 | 0,0501 | 0,0501 | 19,9774 |
| 10 | 0,75 | 1 | 0,3 | 0,3 | 0,3 | 0,3 | 0,0375 | 0,0375 | 26,6366 |
| 11 | 0,75 | 1 | 0,3 | 0,3 | 0,3 | 0,3 | 0,0282 | 0,0282 | 35,5155 |
| 12 | 0,75 | 1 | 0,3 | 0,3 | 0,3 | 0,3 | 0,0211 | 0,0211 | 47,3539 |

The mesh should converge in conditions similar to the Name 12 or finer, in Figure 3.1, the problem is, since it is a 3D complex geometry it takes a long time to make the calculations. Although the results using meshing before converging is not recommended, but it was used because of the computational limitations, deadlines, and the fact that this project seeks to study the relevance of the PDMS film, not the implant geometry itself.

The principal simulations were based on Simulation Name 9 of the Table 3.1. This means that the case without film is exactly like Name 9, and the case with film it has a 0.2 mm Body Size mesh on the film. The simulation will carry with the entire implant. This should provide enough balance between accuracy and processing time, and consequently a good simulation within a reasonable time.
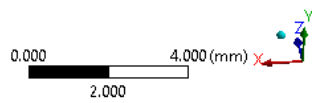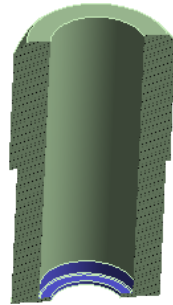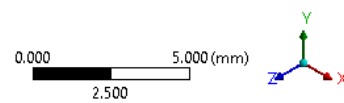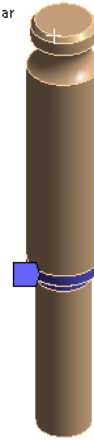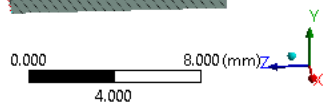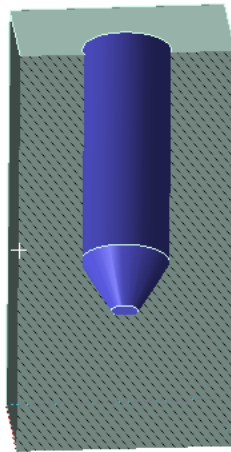
Figure 3.11: Face Sizing of the implant parts.

# Chapter 4

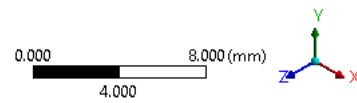# Results and Discussions

This chapter will demonstrate the results achieved in this dissertation whose main objective was the study of a PDMS film wrapped in a dental prosthesis made of titanium as a replacement for lost PDL.

For this, the fundamentals of natural teeth, periodontal ligament, dental implants, titanium, osseointegration, loading conditions, friction, PDMS, and engineering curve were presented.

## 4.1   Specimen

The treatment of data from the tensile test is shown in Figure 4.1, it contains stress of the specimen at each deformation. It is possible to observe that there is an abrupt drop of stress in each graph, which represents the moment when the specimen fails. The first 3 graphics are as expected, with a maximum stress of up to 2 MPa, while the fourth is out of expectation, with a maximum value of almost 3.6 MPa. This discrepancy in the results may consist of a manufacturing error of the specimens since the prepolymer and the hardener have different viscosities and densities, occasionally an incomplete mixture may result in different concentrations. The mechanical characteristics of the PDMS vary according to the concentration of the mixture, that is, there is a possibility that the specimens were not identical, even being from the same batch.
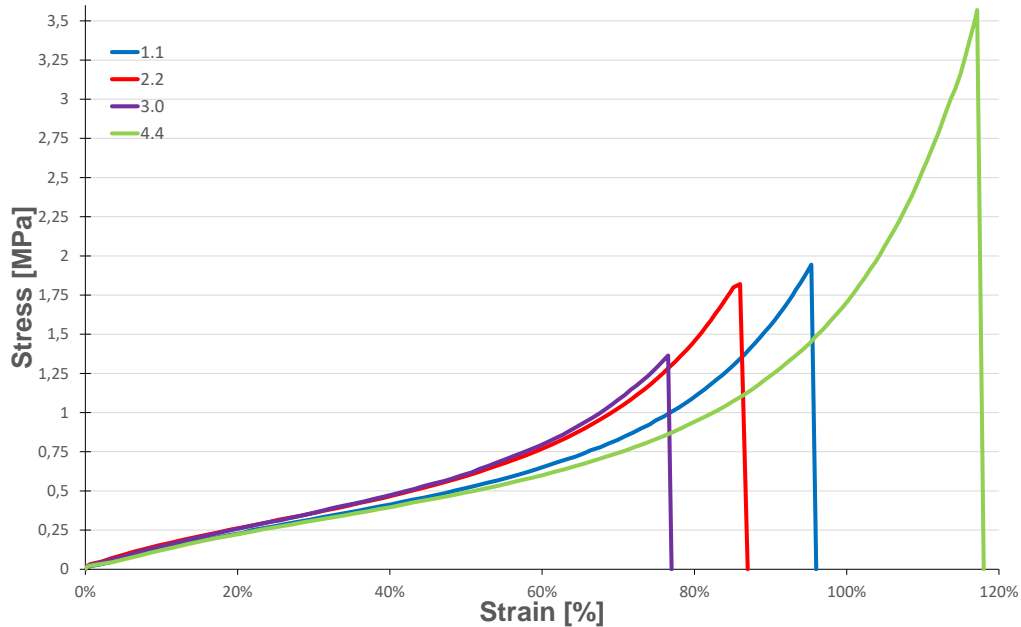
Figure 4.1: Graphic of Stress Strain from data of the tensile tests.

Furthermore, during the tests, slippage of the specimen occurred. The data from tests that slipped were discarded. The PDMS has a smooth surface, the machine claw has shallow engravings that could be resolved with too much grip. However, the specimen would have an unexpected artificial stress concentrator that could alter the results, as it would be crushed too much. Graph curve "1.1" suffered 1 slip, the "2.2" suffered 2 slips, the "3.0" none, and the "4.4" suffered 4 slips.

The virtual tensile test, carried out in the Ansys workbench, demonstrated values that were proximate to the experimental ones with a maximum error of 21.73%. The graph shown in Figure 4.2 shows the relationship between the experimental and virtual behavior of PDMS.
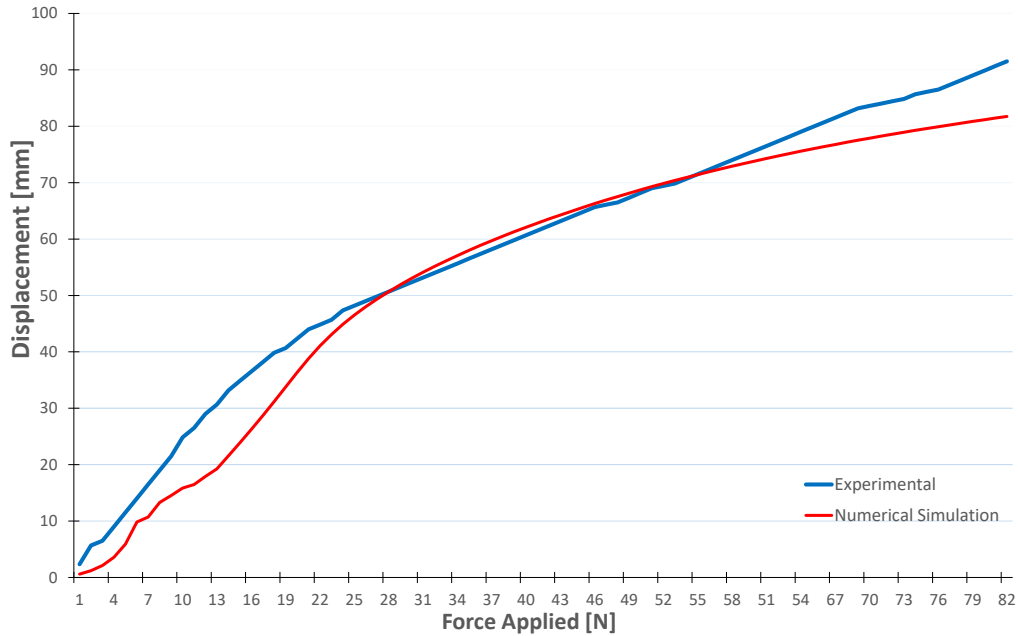
Figure 4.2:   Comparation of Displacement between the experimental tensile test and the numerical one.

## 4.2   Mesh Convergence

Figure 4.3 demonstrates the maximum stresses in relation to each meshing done (for 1/2 implant). The dotted graphs shows the logaritmic trend of each part. The horizontal axis is the inverse of the values of meshing size of the critical faces (F.), found highlighted in the pillar and crown shown in Figure 3.11. It is possible to see that both parts converged or will converge very soon.
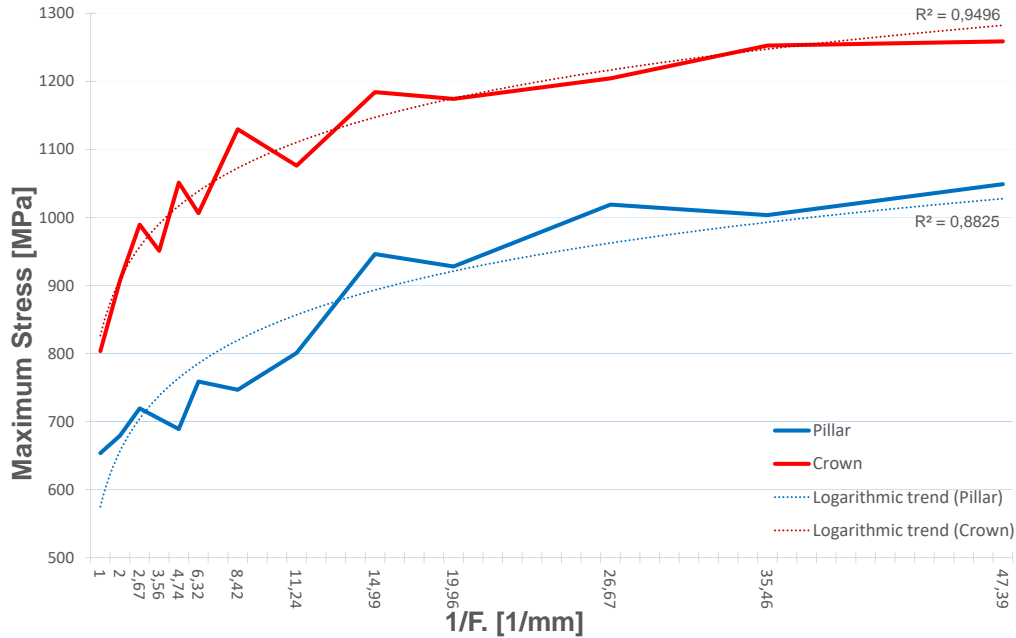
Figure 4.3: Mesh Convergence - Maximum Stress related with meshing.

As already mentioned, it is interesting that any simulation is performed with a sufficiently refined mesh, described by mesh convergence. The present work found that the convergence mesh is too refined for this case because the study geometry is complex. Thus, the ideal simulation would require a lot of processing time and capacity. Even though the simulation does not represent reality perfectly, it is possible to evaluate the effects of the PDMS film on the structure. Therefore, this study is valid.

## 4.3 Implant

The simulation of the entire implant without film at force 133 N, demonstrated Maximum Equivalent Stress (von-Mises) of 723.190 MPa in Crown and Maximum Equivalent Elastic Strain (von-Mises) of $10.322 \times 10^{-3}$ mm/mm in the bone.

Figure 4.4 demonstrates the local Stresses on the Pillar for 133 N, the maximum was

713.220 MPa and $8.275 \times 10^{-3}$ mm/mm. For the Crown, the maximum was 723.130 MPa and $7.867 \times 10^{-3}$ mm/mm, shown in Figure 4.5. Another study that can be highlighted is in the medullar bone, whose values were 14.121 MPa and $10.322 \times 10^{-3}$ mm/mm in the crest, Figure 4.6, the same local as shown in Figure 2.4. The analyze for the screw, is shown in Appendix B, the stress and strain are low, compared to other parts.
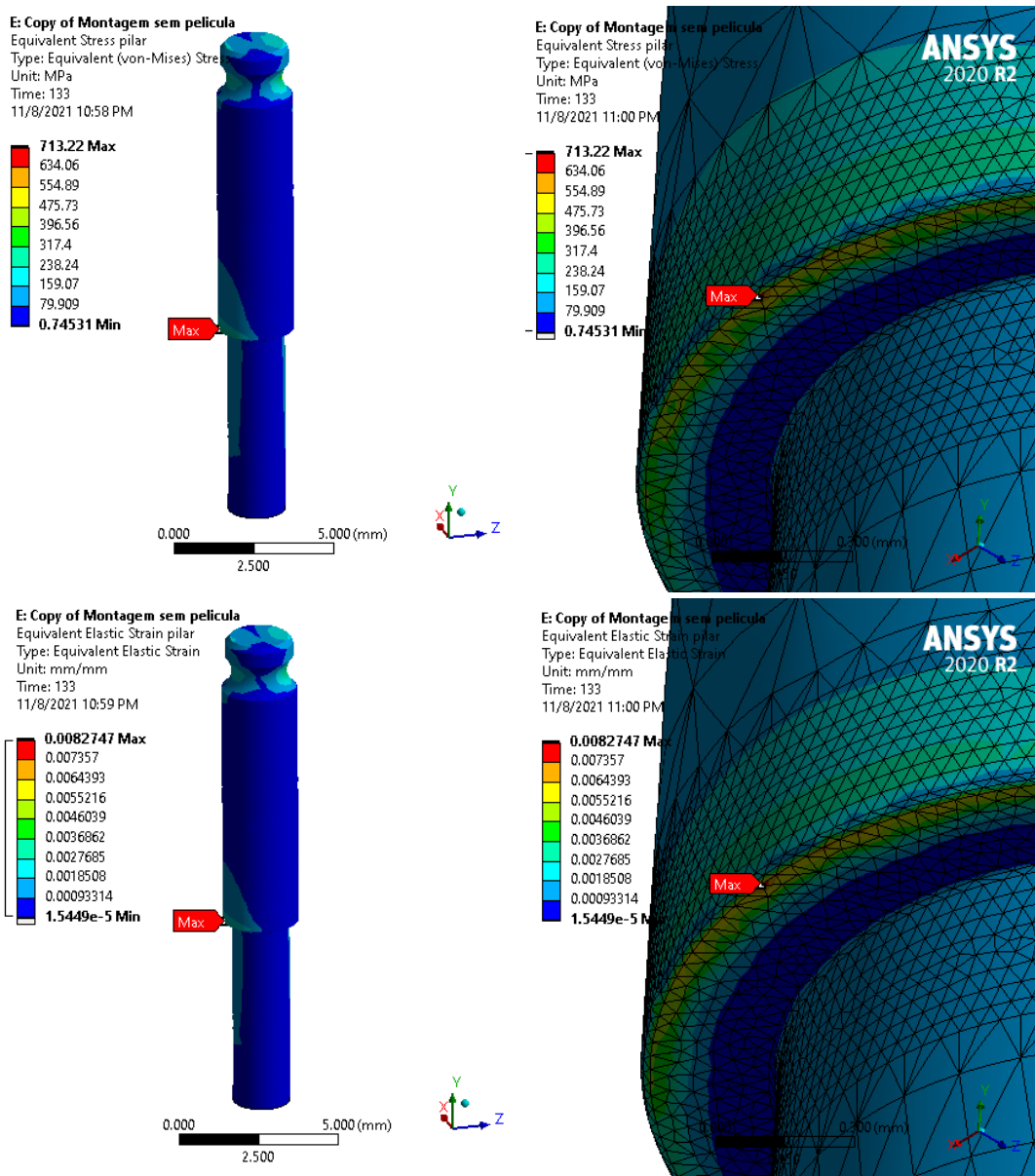


Figure 4.4: Equivalent Stress, with zoom in the critical part, Equivalent Elastic Strain, and with zoom in the critical region of the pillar. Analysis without film.
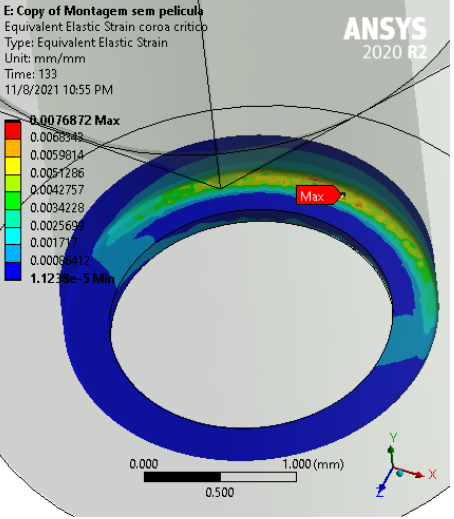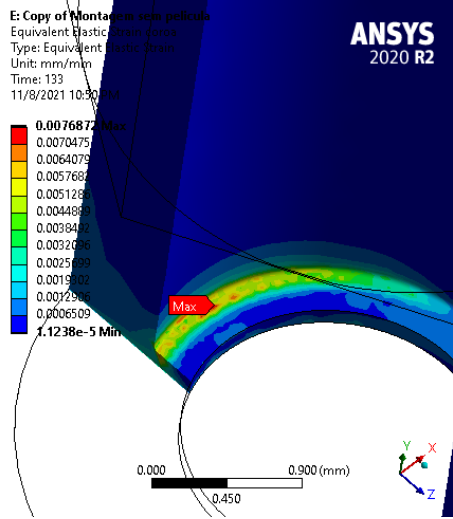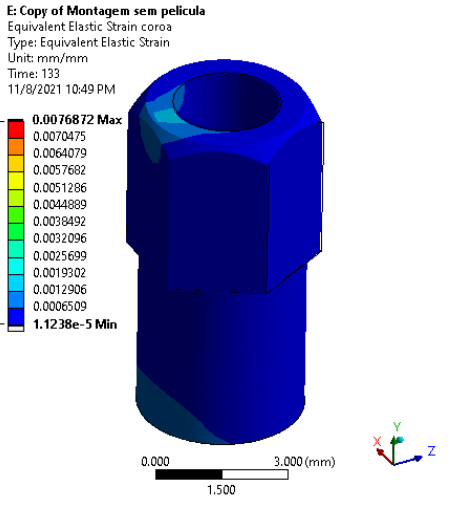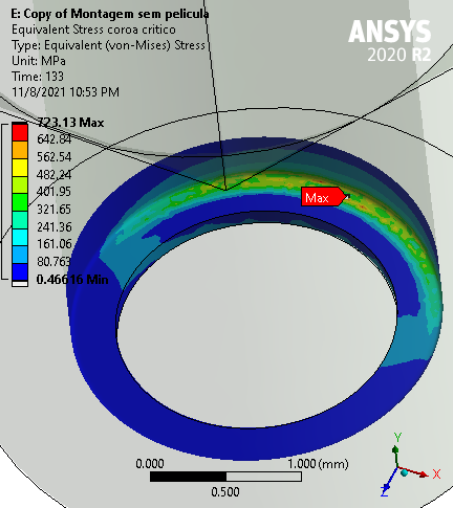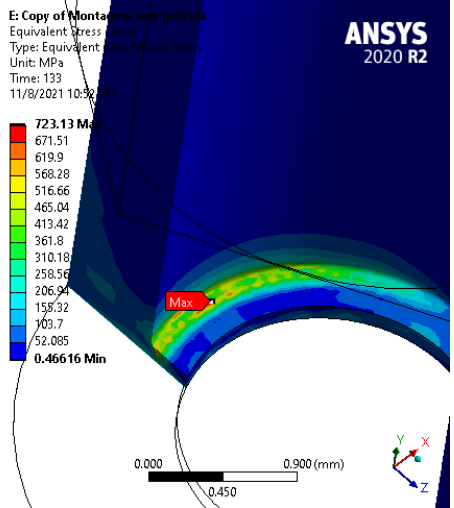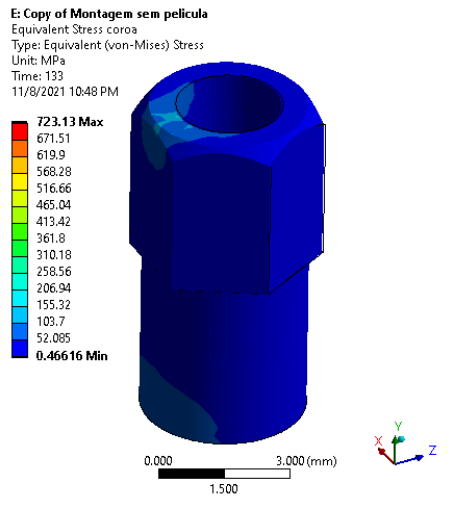
Figure 4.5: Equivalent Stress and Equivalent Elastic Strain, with zoom and cut, and in the critical part of the crown. Analysis without film.
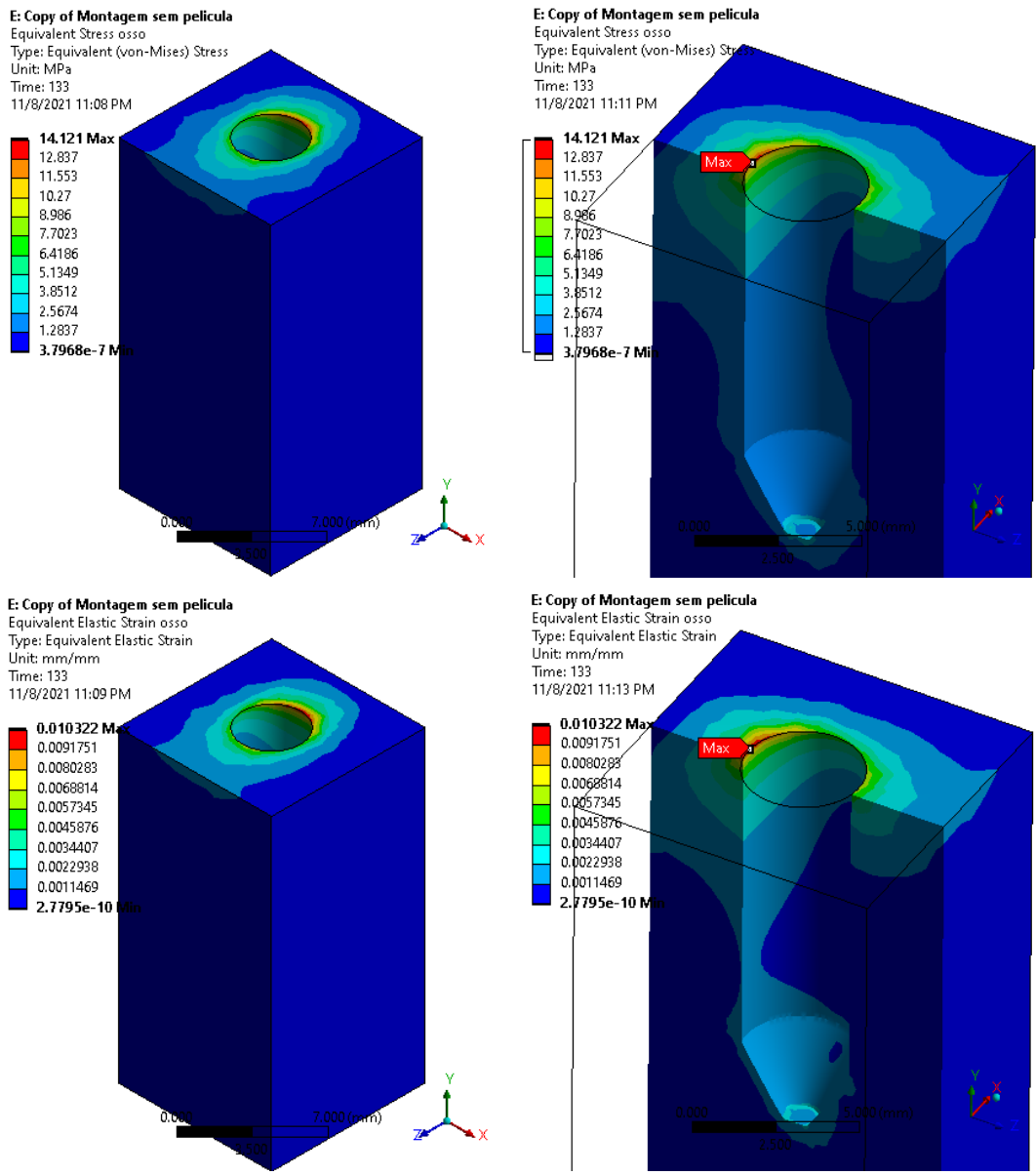
Figure 4.6: Equivalent Stress, with zoom and cut, Equivalent Elastic Strain, and with zoom and cut of the bone. Analysis without film.

Starting with the simulation with PDMS film, it was observed that the Maximum Equivalent Stress (von-Mises) of 681.74 MPa in the Pillar with applied force of 133 N, and Maximum Equivalent Elastic Strain (von-Mises) of 0.278 mm/mm in the PDMS.

The values related to pillar are in Figure 4.7, 681.740 MPa, and $9.145 \times 10^{-3}$ mm/mm.

For the crown however, are 664.130 MPa, and $7.222 \times 10^{-3}$ mm/mm. Finally, for the bone is in Figure 4.8, 14.886 MPa, and $11.596 \times 10^{-3}$ mm/mm.
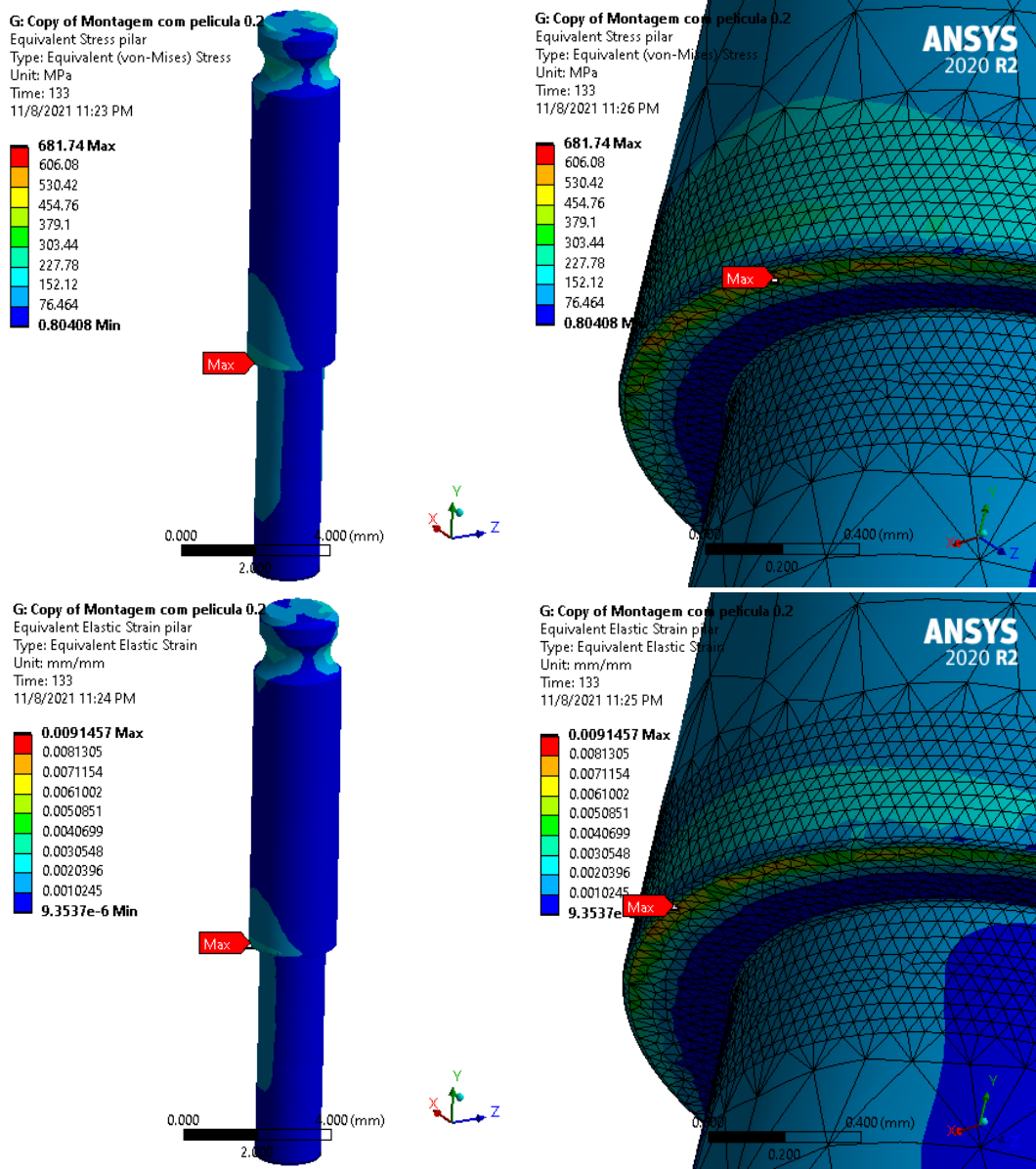


Figure 4.7: Equivalent Stress, with zoom in the critical part, Equivalent Elastic Strain, with zoom in the critical part of the pillar. Analysis with film.
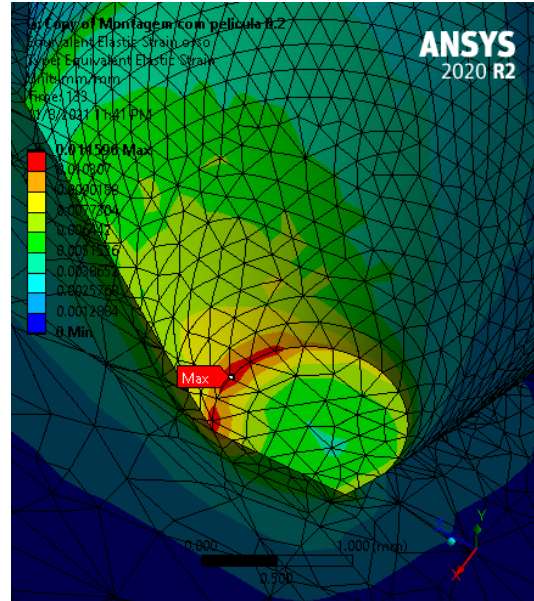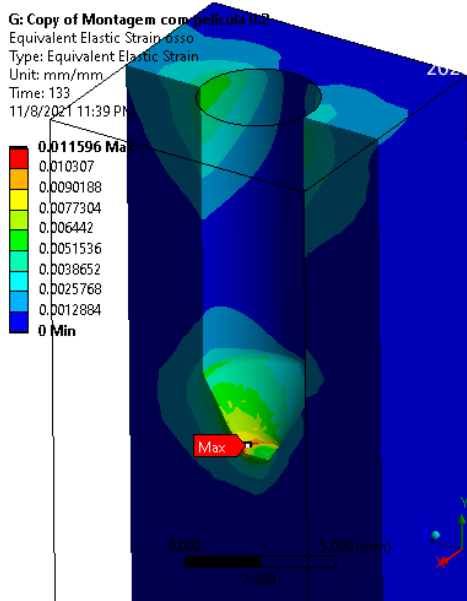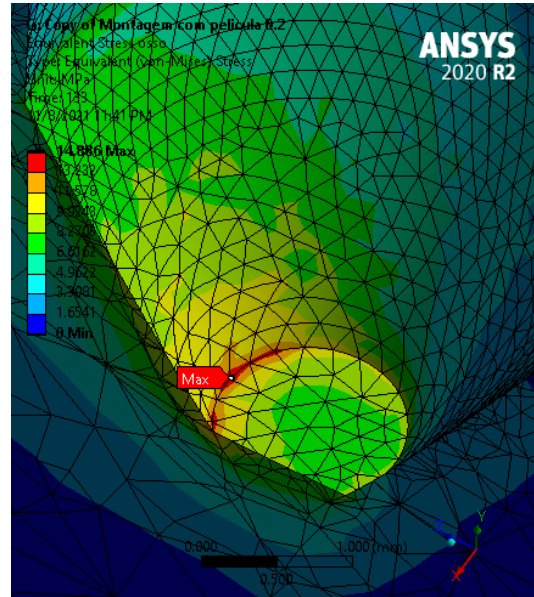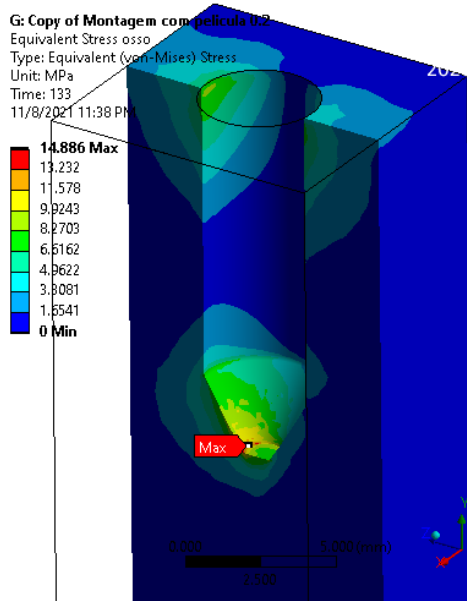
Figure 4.8: Equivalent Stress, with zoom and cut, Equivalent Elastic Strain, and with zoom and cut of the bone. Analysis with film.
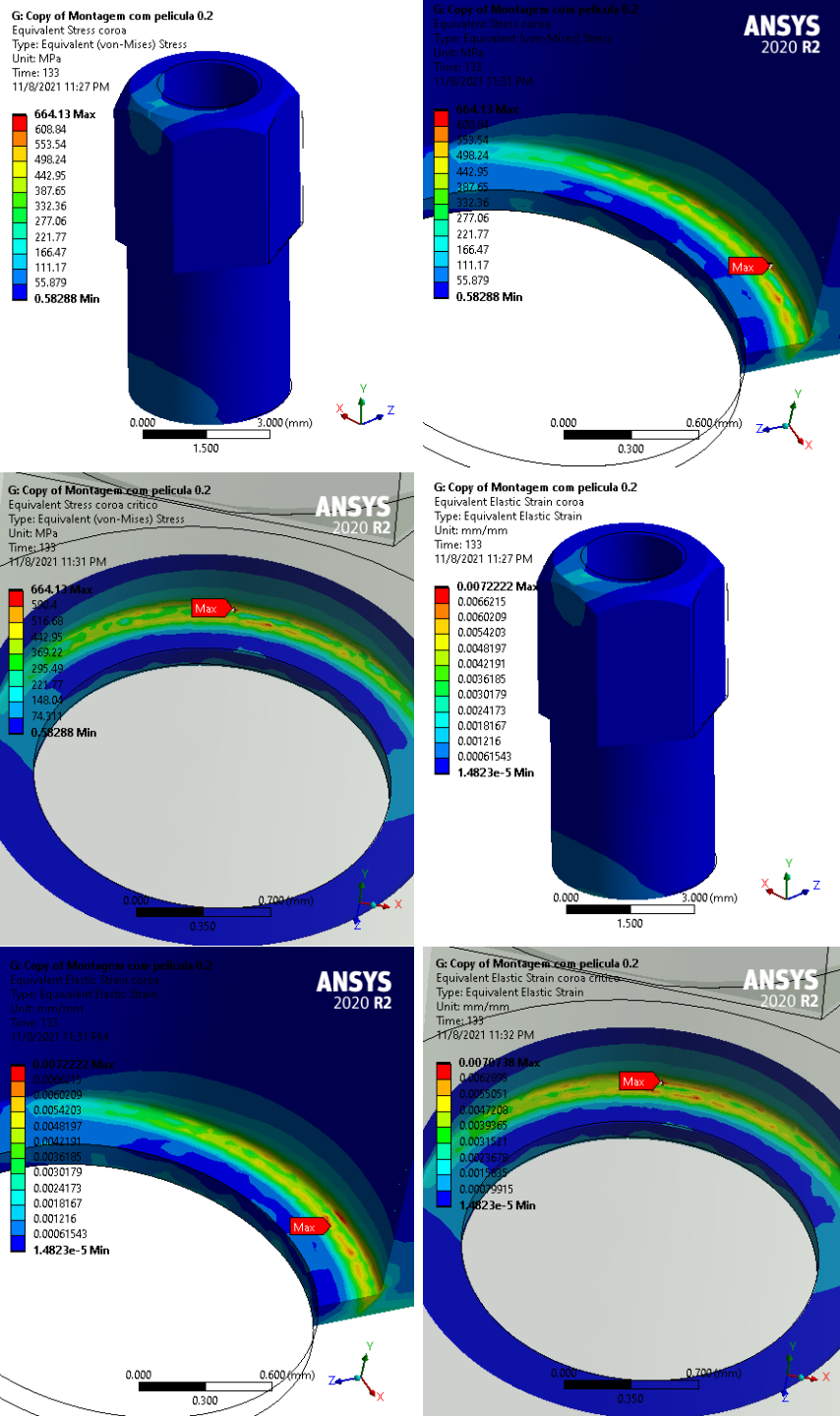
Figure 4.9: Equivalent Stress and Equivalent Elastic Strain, with zoom and cut, and in the critical part of the crown. Analysis with film.

The Equivalent Stress on the bone has not changed much, interestingly, the maximum values changed their location, now in the bottom rather than in the crest. The value that was 14.121 MPa in the crest, turn out to be 8.063 MPa with the adition of PDMS. Similarly for the bottom, that was 3.252 MPa to be 14,886 MPa.

The graph in Figure 4.10 demonstrates a comparison between the value of Equivalent Stress in the Pillar at each increase in force applied. An observed fact is the reduction of the graph's inclination when the force reaches 29 N, for both cases. It can be explained by the deformation of the Pillar in the upper region, which previously had a gap with the crown and does not exist anymore. The top part of the pillar contacts the top part the crown, increasing the rigidity of the model, thus decreasing the rate of stress growth. It is also possible to observe that there is stress in the upper region of the crown, confirming this hypothesis, see Figure 4.5 and 4.9.

As PDMS is a hyperelastic material, one of the expectations is that it anticipates the deformation of the system components, consequently temporarily increasing the stress. From there, it should reduce system stress, acting as a shock absorber. These two hypotheses occur on the pillar, up to 29 N, the stress grows faster with film, but after that, the growth rate decreases compared to standard. At 86 N there is a stress equivalence between the assemblies. See Figure 4.10.

The crown has a similar behavior, however instead of increase the stress until 29 N, it did not changed much, Figure 4.11, after that the growth rate of the stress reduce just like in the pillar, as expected.

Figure 4.13 demonstrates the Equivalent Stress and Equivalent Elastic Strain of the pillar at 29 N. It is possible to observe that the place of greatest equivalent stress has not changed, but as expected the equivalent stress is greater when there is film. Figure 4.14, for the crown, also demonstrates that the equivalent stress location has not changed but a certain proximity of values with or without film, thus confirming the interpretations proposed in Figure 4.10.

For 86 N, only the pillar presents an interesting study since their graphics intersect, for the crown does not present the same behavior. Figure 4.15 demonstrates similar stress and strain values, at this point there is an equivalence of systems.

Lastly, another interesting study should be the deformation that the top face of the pillar had, this way it is possible to see its position varies according to the applied force on the system. Figure 4.12 displays the behavior of implant with the film had a larger deformation in every force, as expected. The growth rate decreases for both of them at 29 N, the same hypothesis shown before.

This study shows the behavior of this implant specifically, it can not be widespread for other geometries. These results may be not be accurate enough because of the rough meshing. That is, maybe if the mesh used is a converged one, the results could be different and bring other discussions and conclusions.
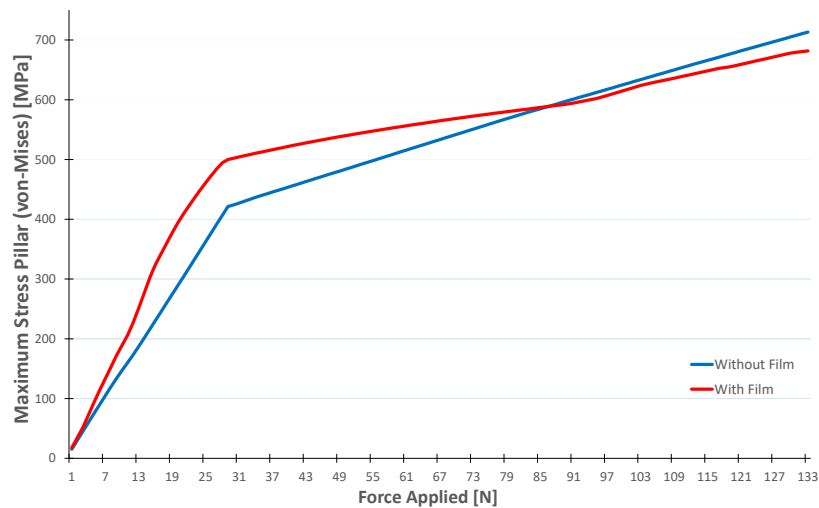


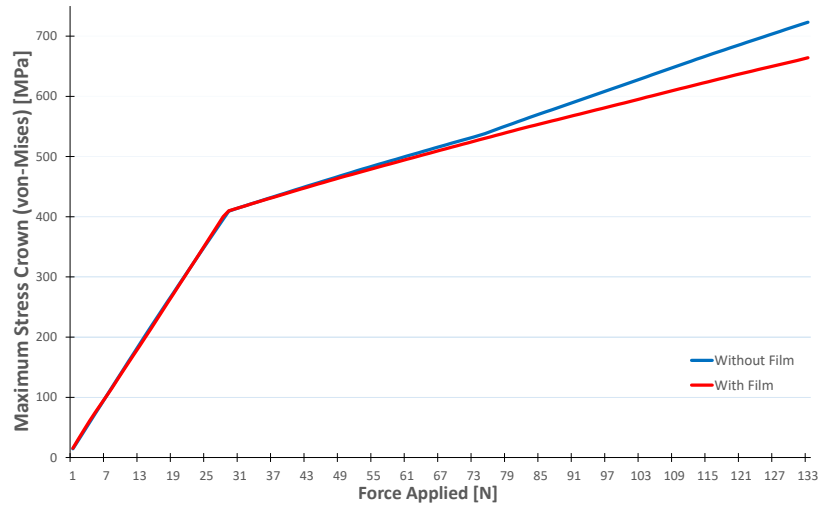Figure 4.10: Maximum Stress in the Pillar versus Applied Force.

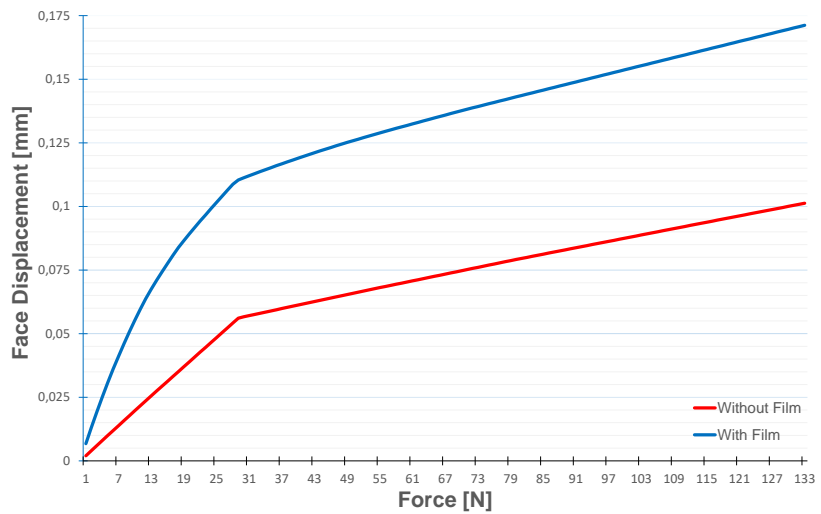Figure 4.11: Maximum Stress in the Crown versus Applied Force.



Figure 4.12: Displacement of the top face of the pillar (with and without film) versus applied force.

Figure 4.13: Equivalent Stress, and Equivalent Elastic Strain of the pillar without film on the top, Equivalent Stress, and Equivalent Elastic Strain of the pillar with film on the bottom. Analysis with force 29 N.

Figure 4.14: Equivalent Stress, and Equivalent Elastic Strain of the crown without film on the top, Equivalent Stress, and Equivalent Elastic Strain of the crown with film on the bottom. Analysis with force 29 N.
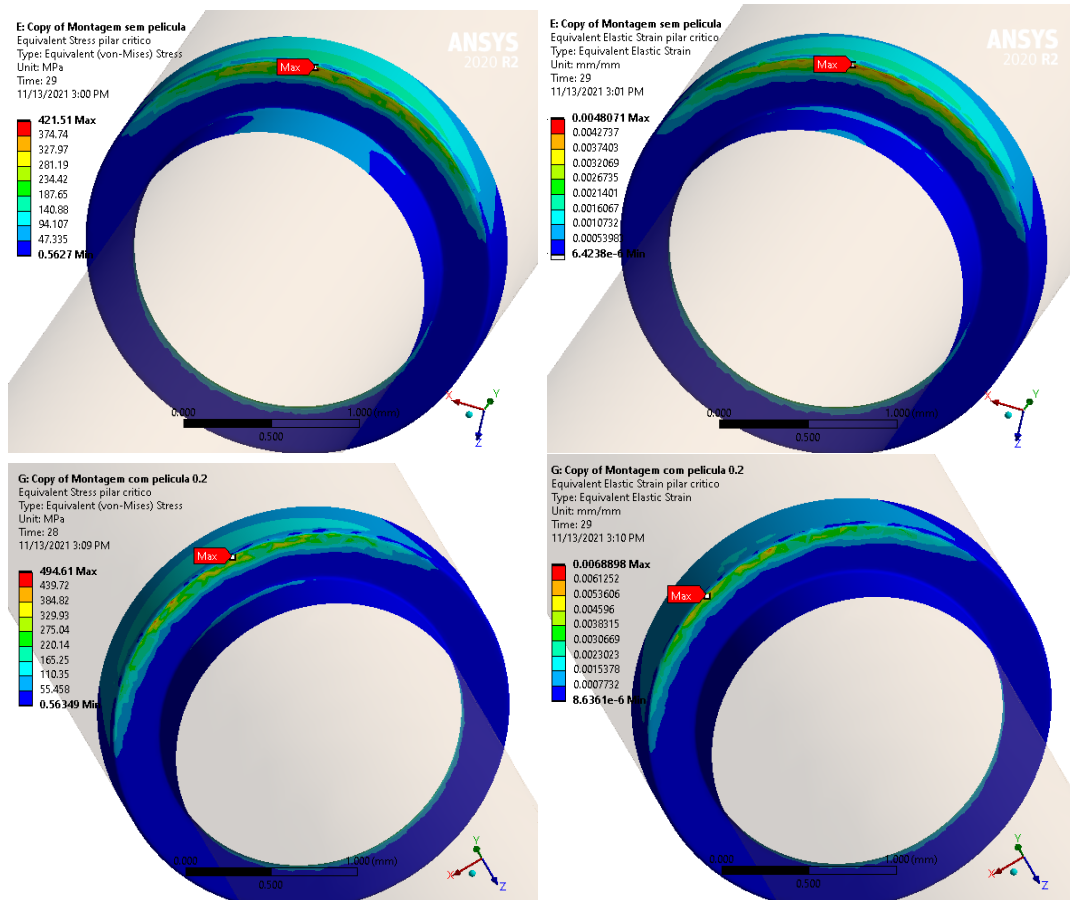
Figure 4.15: Equivalent Stress, and Equivalent Elastic Strain of the pillar without film on the top, Equivalent Stress, and Equivalent Elastic Strain of the pillar with film on the bottom. Analysis with force 86 N.
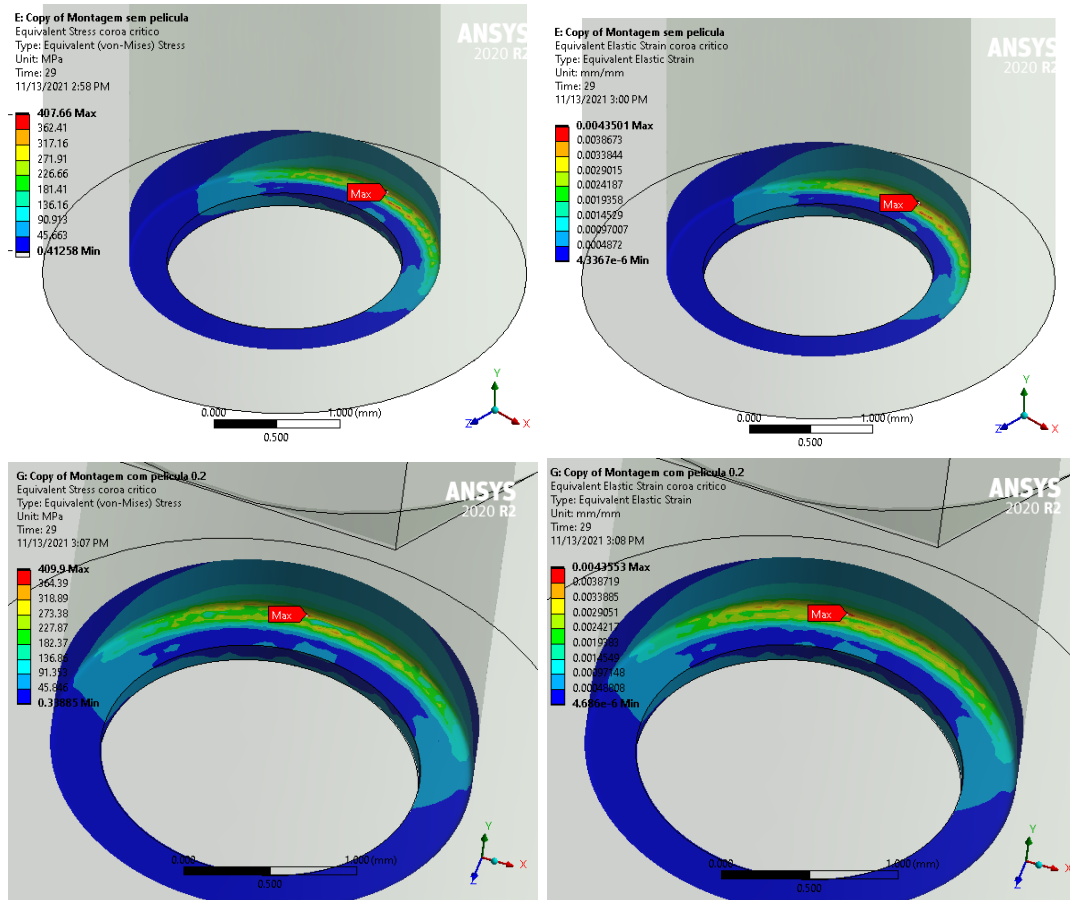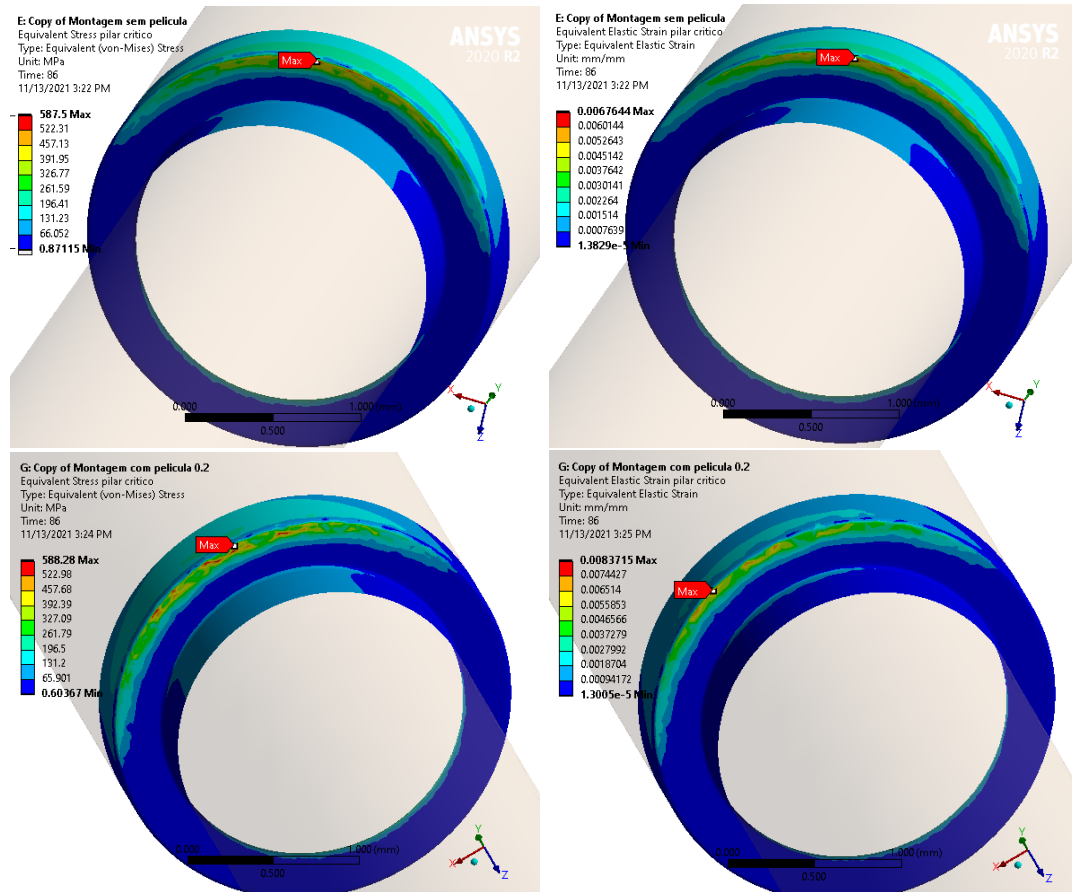
# Chapter 5

# Final Considerations

## 5.1   Conclusion

This research had as general objective to study the behavioral difference between a titanium dental implant prosthesis without periodontal ligament and with an artificial PDL made of PDMS. It was possible to successfully study the behavior of the film as well as the parts of the implant and medullary bone. It was found that in fact, the film made a difference in the numerical simulations.

To support the work more effectively, the authors needed to carry out data acquisitions of the PDMS. So a specific goal is completely related to this important step. Producing and testing the specimen, as well as processing the generated data and performing the test numerically. These goals were achieved successfully.

With the help of the theoretical framework, in different areas, it was possible to simulate and analyze the results of implants from the FEM, even within the limitations found. Thus, the last specific objective was met.

With hyperelastic behavior, the hypothesis was that it would act as a shock absorber, partially absorbing mechanical energy deposited on the tooth crest. This hypothesis was confirmed since the present study showed that the film generates a decrease in stress. The increase in stress in the pillar is caused by the high strain provided by the film until the

top contact occurs between pillar and crown, this means that if the gap did not exist, the pillar would behave the same as the crown.

The addition of the film changed the behavior of the bone as well, previously it had its highest stress in the crest and changed to the bottom of the bone. This shows that the PDMS distributed better the stress on the bone. Within a limited scope, the PDMS acted as expected, behaving like a kind of periodontal ligament.

However, the problem was not totally solved, other characteristics were not studied in this work as a substitute for the PDL. It is possible to highlight that properties such as movement, useful life, thermal and electrical conductors, expansion, among others, are still to be studied for this specific objective. So it is too early to conclude that a PDMS film is a definitive replacement for PDL, but it does indicate that it is a strong candidate.

During this work, several limitations were found, including few specimens may not have sufficiently reduced the error related to manufacturing failures; little variety of concentrations between prepolymer and hardener, it would be interesting to see if other proportions have more adequate characteristics; few tensile tests to reduce test error; slip of the specimens during the tensile test; dimensions taken from an implant on an enlarged scale, can add errors to the process of reducing the model; study of a single implant model, this implant may not be suitable for the application of a film that is not seen in the project, which may compromise its performance; study of a single film thickness, nothing indicates that this thickness is ideal, perhaps thinner or even greater; insufficiently refined meshes can and probably will negatively compromise results; computer with limited processing capacity, limitate some parameters of the simulation, like the mesh refinement.

## 5.2   Future Works

As an indication for academics who read this work, is the solution or attenuation of the limitations raised above, namely, increase the number of specimens, more tensile test, resolve the slipping of the specimens during the test within the ASTM Standard, work on a 3D CAD model received from a certified designer or dental implant factory, study more

implants with different geometry, study various thickness of the film, study the behavior change of the hyperelastic solvers method in this system, use finer meshing, and use an excellent computer or cluster for simulations.

# Bibliography

[1]  B. M. Nigg, *Biomechanics of the musculo-skeletal system*. John Wiley & Sons Incorporated, 2007, ISBN: 9780470017678.

[2]  A. A. Caputo and J. P. Standlee, *Biomechanics in clinical dentistry*. Chicago: Quintessence Publishing Co, 1987, ISBN: 9780867151787.

[3]  Fortune Bussines Insight, *Dental implants market size, share and covid-19 impact analysis*, https://www.fortunebusinessinsights.com/industry-reports/dental-implants-market-100443, Accessed: 2021-11-30, 2021.

[4]  N. Miller, "Ten cate's oral histology," *British Dental Journal*, vol. 213, no. 4, pp. 194–194, 2012.

[5]  J. Kinney, S. Marshall, and G. Marshall, "The mechanical properties of human dentin: A critical review and re-evaluation of the dental literature," *Critical Reviews in Oral Biology & Medicine*, vol. 14, no. 1, pp. 13–29, 2003.

[6]  B. Berkovitz, "The structure of the periodontal ligament: An update," *The European Journal of Orthodontics*, vol. 12, no. 1, pp. 51–76, 1990.

[7]  N. D. Mohl and J. D. Rugh, *A Textbook of Occlusion*. Illinois: Quintessence, 1988, ISBN: 9780867151671.

[8]  P. W. Lucas, *Dental Functional Morphology How Teeth Work*. UK: Cambridge University Press, 2010, ISBN: 9780521562362.

[9] J. Boldt, W. Knapp, P. Proff, K. Rottner, and E.-J. Richter, "Measurement of tooth and implant mobility under physiological loading conditions," *Annals of Anatomy-Anatomischer Anzeiger*, vol. 194, no. 2, pp. 185–189, 2012.

[10] L. Mioche and M.-A. Peyron, "Bite force displayed during assessment of hardness in various texture contexts," *Archives of Oral Biology*, vol. 40, no. 5, pp. 415–423, 1995.

[11] C. Misch and M. Bidez, "Considerações oclusais para a prótese implanto suportada: Oclusão implanto protegida," *Elsevier*, pp. 472–510, 2006.

[12] S. Gomes de Oliveira, P. Seraidarian, J. Landre Jr, D. Oliveira, and B. Cavalcanti, "Tooth displacement due to occlusal contacts: A three-dimensional finite element study," *Journal of oral rehabilitation*, vol. 33, no. 12, pp. 874–880, 2006.

[13] Colgate, *Ligamento periodontal: O que é?* `https://www.colgate.com.br/oral-health/mouth-and-teeth-anatomy/periodontal-ligament--what-is-it`, Accessed: 2021-08-08, 2015.

[14] S. Standring, *Gray's Anatomy The Anatomical Basis of Clinical Practice*. Elsevier, 2020, ISBN: 9780443066757.

[15] N. D. E. Varanda, "Ligamento periodontal e síntese de colagénio estudo experimental," M.S. thesis, Faculdade de Medicina da Universidade de Coimbra, Coimbra, PT, 2010.

[16] P. Sloan, "Collagen fibre architecture in the periodontal ligament," *Journal of the Royal Society of Medicine*, vol. 72, no. 3, pp. 188–191, 1979.

[17] R. J. Genco, A. W. Ho, J. Kopman, S. G. Grossi, R. G. Dunford, and L. A. Tedesco, "Models to evaluate the role of stress in periodontal disease," *Annals of Periodontology*, vol. 3, no. 1, pp. 288–302, 1998.

[18] Neodent, "Catálogo neodent," 2021.

[19] C. Misch, *Implantes Dentais Contemporâneos*. Elsevier, 2009, ISBN: 9781336261754.

[20] Conceição, Ewerton Nocchi, *Pino intrarradicular de fibra: A revolução da qualidade, agilidade e estética*, `http://www.angelus.ind.br/artigo-publicacao/pino-intra-radicular-de-fibra:-a-revolucao-da-qualidade,-agilidade-e-estetica/243`, Accessed: 04-05-2019, 2016.

[21] MatWeb, *Matweb, your source for materials informationa*, `http://www.matweb.com/index.aspx`, Accessed: 04-08-2021.

[22] Straumann, `https://straumannprod-h.assetsadobe2.com/is/image/content/dam/sites/neodent/br/pacientes/lp_beneficios/Beneficios_2_Sobre-Imagem.jpg?wid=720`, Accessed: 2021-08-06.

[23] M. CE, *Implantes dentários contemporâneos*. São Paulo, SP: Ed.Santos, 2000, ISBN: 9788535246094.

[24] V. M. et al., "Osseointegração: Análise de fatores clínicos de sucesso e insucesso," *Revista Odontológica de Araçatuba*, vol. 32, no. 1, pp. 26–31, 2011.

[25] M. F. A. et al., "Resistance to maxillary premolar fractures after restoration of class ii preparations with resin composite or ceromer," *Quintessence International-English Edition*, vol. 33, no. 8, pp. 589–594, 2002.

[26] S. R. Braga C Mezzomo E, "Resistência à fratura de três sistemas de prótese parcial fixa livres de metal, estudo in vitro," *PCL*, vol. 6, no. 31, pp. 249–261, 2004.

[27] J. C. M. S. et al., "A comprehensive review on the corrosion pathways of titanium dental implants and their biological adverse effects," *Metals (MDPI)*, vol. 10, no. 9, 2020.

[28] Aline Iohann, `https://alineiohann.odo.br/wp-content/uploads/2019/05/Implante-dentário-pagina.jpg`, Accessed: 2021-07-08.

[29] M. A. N Wakabayashi 1 H Mizutani, "All-cast-titanium removable partial denture for a patient with a severely reduced interarch distance: A case report," *Quintessence Int*, vol. 28, no. 3, pp. 173–6, 1997.

[30]  K. Wang, "The use of titanium for medical applications in the usa," *Materials Science and Engineering: A*, vol. 213, no. 1-2, pp. 134–137, 1996.

[31]  F. J. P. Modaffore PM Kliemann C, "Liga metálica de titânio: Uma nova alternativa na confecção das armações em prótese parcial removível?" *PCL*, vol. 3, no. 15, pp. 421–430, 2001.

[32]  J. T. B. et al., "Comparison of titanium and cobalt-chromium removable partial denture clasps," *PCL*, vol. 78, no. 2, pp. 187–93, 1997.

[33]  Fort Wayne Metals Research Products Corp - FWMetals, *Ti 6al-4v eli*, `https://www.fwmetals.com/services/resource-library/ti-6al-4v-eli/`, Accessed: 2021-08-25.

[34]  J. R. Patterson EA, "Theoretical analysis of the fatigue life of fixture screws in osseointegrated dental implants.," *The International Journal of Oral Maxillofacial Implants*, vol. 7, no. 1, pp. 26–33, 1992.

[35]  R. B. et al., "Influence of hex geometry and prosthetic table width on static and fatigue strength of dental implants," *The Journal of Prosthetic Dentistry*, vol. 82, no. 4, pp. 436–440, 1999.

[36]  T. G. et al., "Probabilistic analysis of preload in the abutment screw of a dental implant complex," *The Journal of Prosthetic Dentistry*, vol. 100, no. 3, pp. 183–193, 2008.

[37]  H. J. McGlumphy EA Mendel DA, "Implant screw mechanics," *Dental Clinics of North America*, vol. 42, no. 1, pp. 71–89, 1998.

[38]  J. Lindhe, T. Karring, and N. P. Lang, *Clinical periodontology and implant dentistry.* Blackwell, 2003, ISBN: 9781118682067.

[39]  e. a. I. Fasaki K. Siamos, "Ultrasound assisted preparation of stable water-based nanocrystalline tio2 suspensions for photocatalytic applications of inkjet-printed films," *Applied Catalysis A: General*, vol. 411, pp. 60–69, 2012.

[40] F. Groch, "Biomecânica da prótese implanto-suportada: Uma revisão de conceitos," M.S. thesis, Universidade Federal do Rio Grande do Sul, Porto Alegre, RS, Brazil, 2010.

[41] D. L. Dixon, L. C. Breeding, J. P. Sadler, and M. L. McKay, "Comparison of screw loosening, rotation, and deflection among three implant designs," *The Journal of prosthetic dentistry*, vol. 74, no. 3, pp. 270–278, 1995.

[42] R. Skalak, "Biomechanical considerations in osseointegrated prostheses.," *The Journal of prosthetic dentistry*, vol. 49, no. 6, pp. 843–848, 1983.

[43] T. Flügge, W. J. van der Meer, B. G. Gonzalez, K. Vach, D. Wismeijer, and P. Wang, "The accuracy of different dental impression techniques for implant-supported dental prostheses: A systematic review and meta-analysis," *Clinical oral implants research*, vol. 29, pp. 374–392, 2018.

[44] J. A. Lopes Júnior, "Análise numérica de interfaces de próteses dentárias através da mecânica do dano," Ph.D. dissertation, Universidade Estadual Paulista (UNESP), Bauru, São Paulo, Brazil, 2012.

[45] Maia Odontologia, `https://maiaodontologia.com.br/p8027.aspx`, Accessed: 2020-12-10.

[46] A. M. O'Mahony, J. L. Williams, J. O. Katz, and P. Spencer, "Anisotropic elastic properties of cancellous bone from a human edentulous mandible," *Clinical oral implants research*, vol. 11, no. 5, pp. 415–421, 2000.

[47] C. S. R. Leopoldo Daniel Moreira Tavares Carlos Alberto Fonzar Pintão, "Coeficientes de atrito estático e dinâmico com amostras de titânio," in *XXVI Congresso de Iniciação Científica da UNESP*, 2014.

[48] G. Lorenz and A. Kandelbauer, "Silicones," in *Handbook of Thermoset Plastics*, Elsevier, 2014, pp. 555–575, ISBN: 9781455731091.

[49] J. K. Fink, *Reactive polymers: fundamentals and applications: a concise guide to industrial polymers*. William Andrew, 2017, ISBN: 9781455731589.

[50]  T. Guélon, E. Toussaint, J.-B. Le Cam, N. Promma, and M. Grediac, "A new characterisation method for rubber," *Polymer testing*, vol. 28, no. 7, pp. 715–723, 2009.

[51]  P. Wexler, *Encyclopedia of toxicology.* Elsevier/Academic Press, 2014, ISBN: 9780127453552.

[52]  Fanse, "Effect of crosslinking on the physicochemical properties of polydimethylsiloxane-based levonorgestrel intrauterine systems," *International journal of pharmaceutics*, vol. 609, p. 121 192, Oct. 2021.

[53]  A. Ainla, "Valves for microfluidic devices," M.S. thesis, Chalmers University of Technology, Göteborg, Sweden, 2007.

[54]  R. Ariati, F. Sales, A. Souza, R. A. Lima, and J. Ribeiro, "Polydimethylsiloxane composites characterization and its applications: A review," *Polymers*, vol. 13, no. 23, p. 4258, 2021. DOI: `10.3390/polym13234258`.

[55]  F. S. A. Andrews Victor João Ribeiro, "Study of pdms characterization and its applications in biomedicine: A review," *Journal of Mechanical Engineering and Biomechanics*, vol. 4, pp. 1–9, Jul. 2019.

[56]  A. Souza, M. S. Souza, D. Pinho, *et al.*, "3d manufacturing of intracranial aneurysm biomodels for flow visualizations: Low cost fabrication processes," *Mechanics Research Communications*, vol. 107, p. 103 535, 2020.

[57]  J. S. Park, R. Cabosky, Z. Ye, and I. I. Kim, "Investigating the mechanical and optical properties of thin pdms film by flat-punched indentation," *Optical Materials*, vol. 85, pp. 153–161, 2018.

[58]  H. Montazerian, M. Mohamed, M. M. Montazeri, *et al.*, "Permeability and mechanical properties of gradient porous pdms scaffolds fabricated by 3d-printed sacrificial templates designed with minimal surfaces," *Acta biomaterialia*, vol. 96, pp. 149–160, 2019.

[59]  T. J. Keane and S. F. Badylak, "Biomaterials for tissue engineering applications," in *Seminars in Pediatric Surgery*, Elsevier, vol. 23, 2014, pp. 112–118.

[60]  Y. Shi, M. Hu, Y. Xing, and Y. Li, "Temperature-dependent thermal and mechanical properties of flexible functional pdms/paraffin composites," *Materials & Design*, vol. 185, pp. 108–219, 2020.

[61]  R. Giri, K. Naskar, and G. B. Nando, "Effect of electron beam irradiation on dynamic mechanical, thermal and morphological properties of lldpe and pdms rubber blends," *Radiation physics and chemistry*, vol. 81, no. 12, pp. 1930–1942, 2012.

[62]  F. Pereira Sales, A. Souza, R. Ariati, *et al.*, "Composite material of pdms with interchangeable transmittance: Study of optical, mechanical properties and wettability," *Journal of Composites Science*, vol. 5, p. 110, Apr. 2021. DOI: `10.3390/jcs5040110`.

[63]  N. R. P. Moreira, "Estudo de várias propriedades mecânicas do polidimetilsiloxano (pdms) usado em dispositivos biomédicos," Ph.D. dissertation, ESTiG - School of Technology and Management, Polytechnic Institute of Bragança, Bragança, Portugal, 2013.

[64]  J. E. Ribeiro, H. Lopes, P. Martins, and M. Braz-César, "Mechanical analysis of pdms material using biaxial test," *AIMS Materials Science*, vol. 6, no. 1, pp. 97–110, 2019.

[65]  S. R. Alvaro Mata Aaron J. Fleischman, "Characterization of polydimethylsiloxane (pdms) properties for biomedical micro/nanosystems," *Biomedical microdevices*, vol. 7, no. 4, pp. 281–293, 2005.

[66]  A. Öchsner, L. F. M. da Silva, and H. Altenbach, *Materials with Complex Behaviour II*. Springer, 2012, ISBN: 9783642227004.

[67]  M. D. Banea and L. F. da Silva, "Mechanical characterization of flexible adhesives," *The Journal of Adhesion*, vol. 85, no. 4-5, pp. 261–285, 2009.

[68]  Instron, *Modulos of elasticity*, `http://www.instron.com.br/wa/glossary/Modulus-of-Elasticity.aspx`, 2010.

[69] Autodesk Sustainable Product Design, *Metrics and the basics of mechanics - part 2*, `https://knowledge.autodesk.com/search-result/caas/simplecontent/content/metrics-and-the-basics-mechanics-part-2.html`, Accessed: 2021-11-24.

[70] Sazzad, MM and Rahman, FI and Mamun, MAA, "Mesh effect on the fem based stability analysis of slope," in *International Conference on Recent Innovation in Civil Engineering for Sustainable Development (IICSD-2015)*, 2015, pp. 387–391.

[71] S. Oberhollenzer, F. Tschuchnigg, and H. F. Schweiger, "Finite element analyses of slope stability problems using non-associated plasticity," *Journal of Rock Mechanics and Geotechnical Engineering*, vol. 10, no. 6, pp. 1091–1101, 2018.

[72] K. S. Rezende, "Estudos de caso: Teste de convergência de malha e comparações entre equilıbrio limite e análise de tensão-deformação em estabilidade de taludes aplicada a minas a céu aberto," M.S. thesis, Universidade Federal de Viçosa, Viçosa, Minas Gerais, Brazil, 2020.

[73] G. R. Bhashyam, "Ansys mechanical—a powerful nonlinear simulation tool," *Ansys, Inc*, vol. 1, no. 1, p. 39, 2002.

# Appendix A

# Surface Contacts
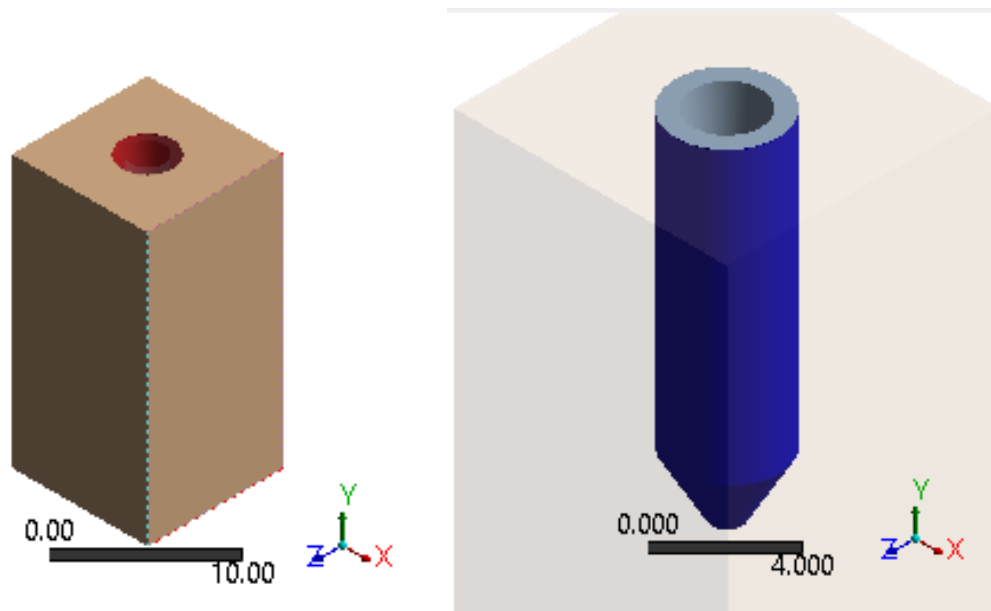
Figure A.1: Connection 1. The bone is in the left and the screw on the right.
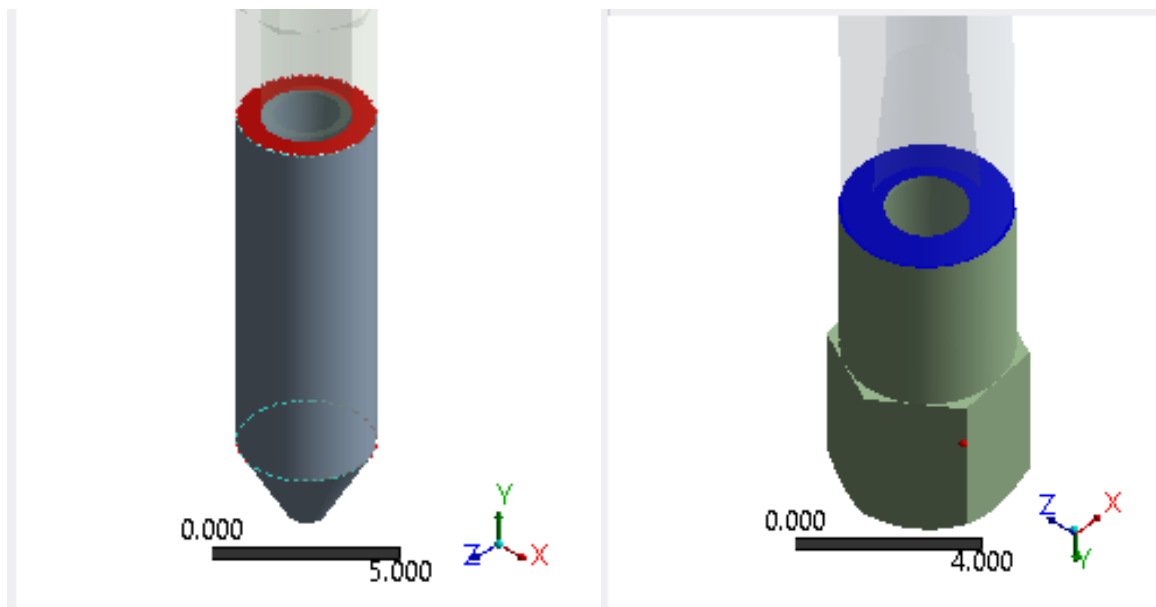


Figure A.2: Connection 2: The screw is on the left and the crown on the right upside down.
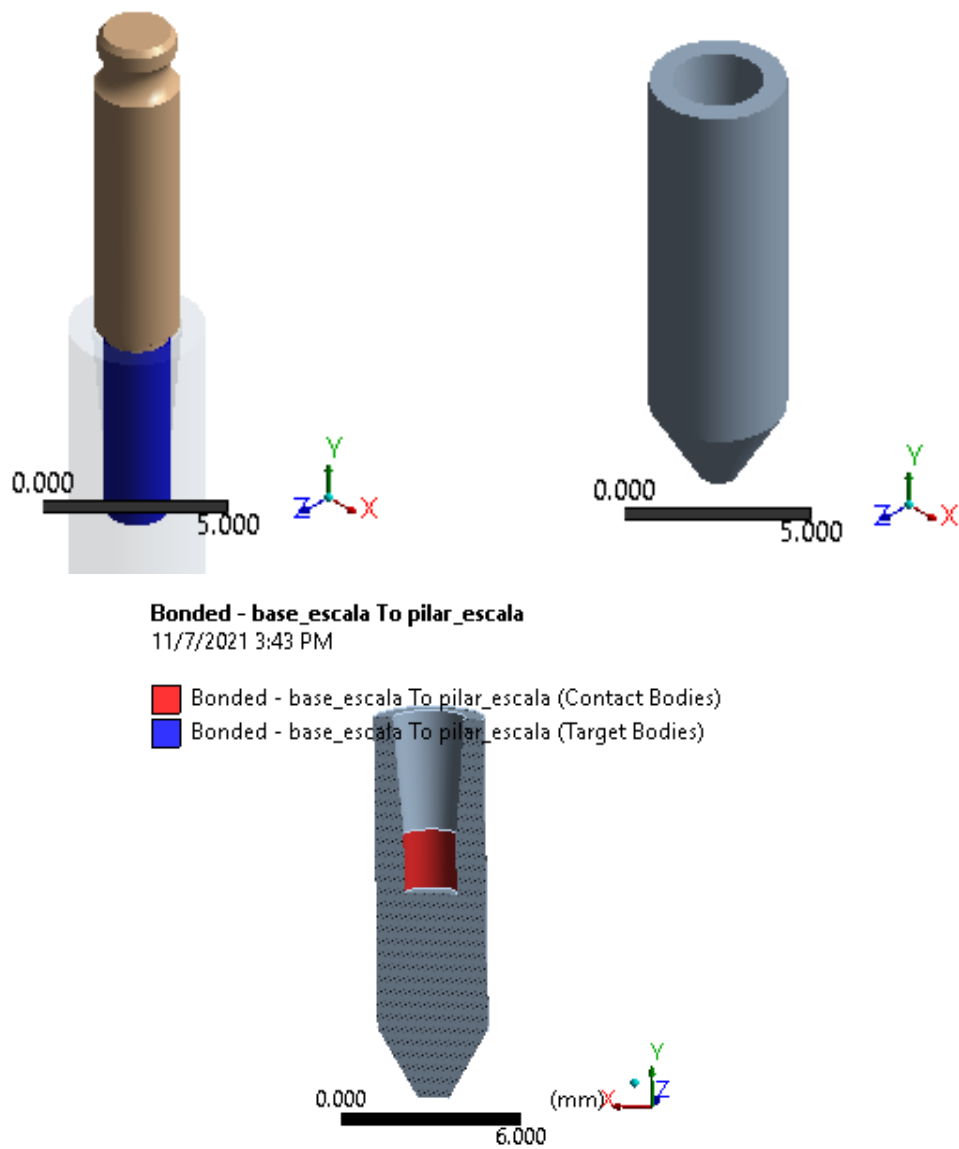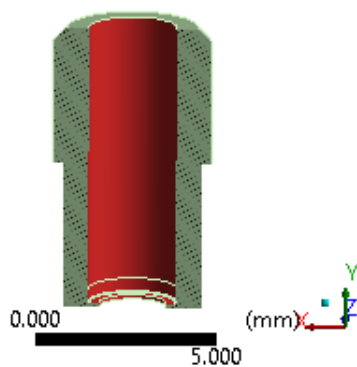
Figure A.3: Connection 3: The pillar is on the top left corner, the screw on the top right corner, and in the bottom center is the screw cut in half.
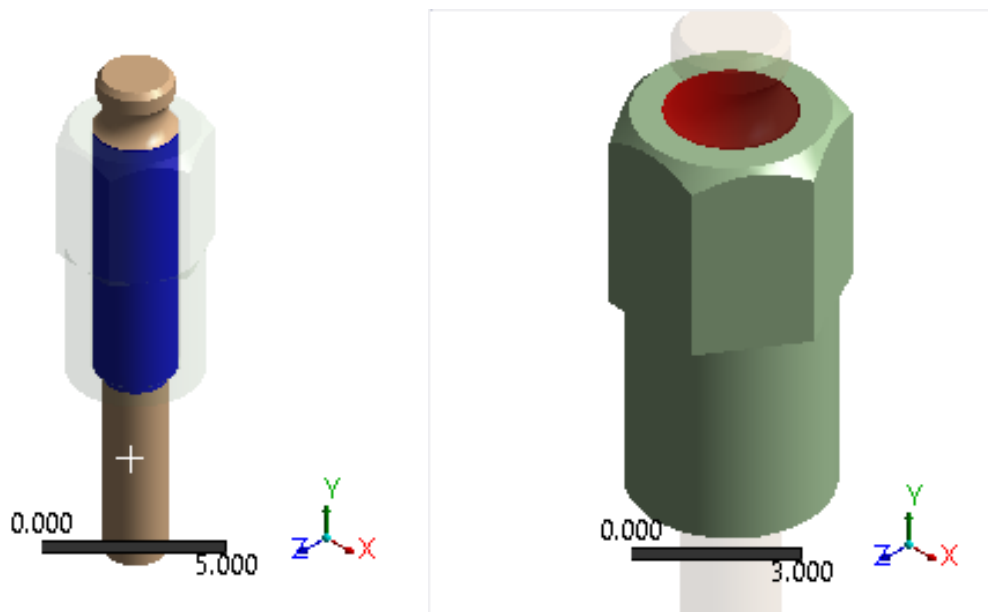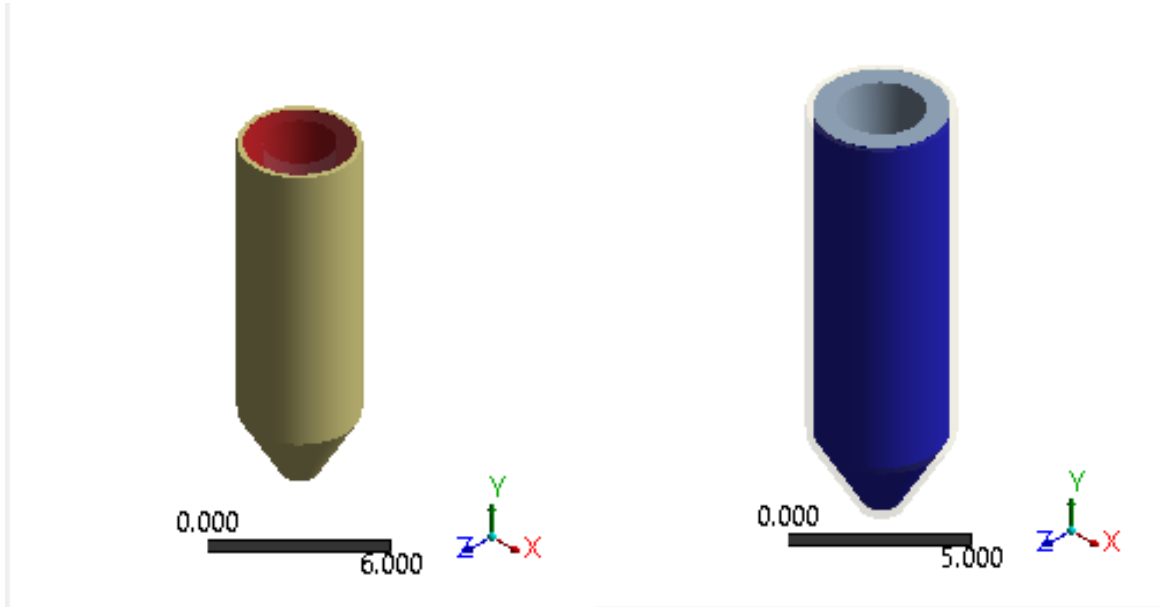
Frictional - coroa_escala To pilar_escala
11/7/2021 3:45 PM

Frictional - coroa_escala To pilar_escala (Contact Bodie:
Frictional - coroa_escala To pilar_escala (Target Bodies)

Figure A.4: Connection 4: The pillar is on the top left corner, the crown on the top right corner, and in the bottom center is the crown cut in half

Figure A.5: Connection 5. The PDMS film is in the left and the screw on the right.
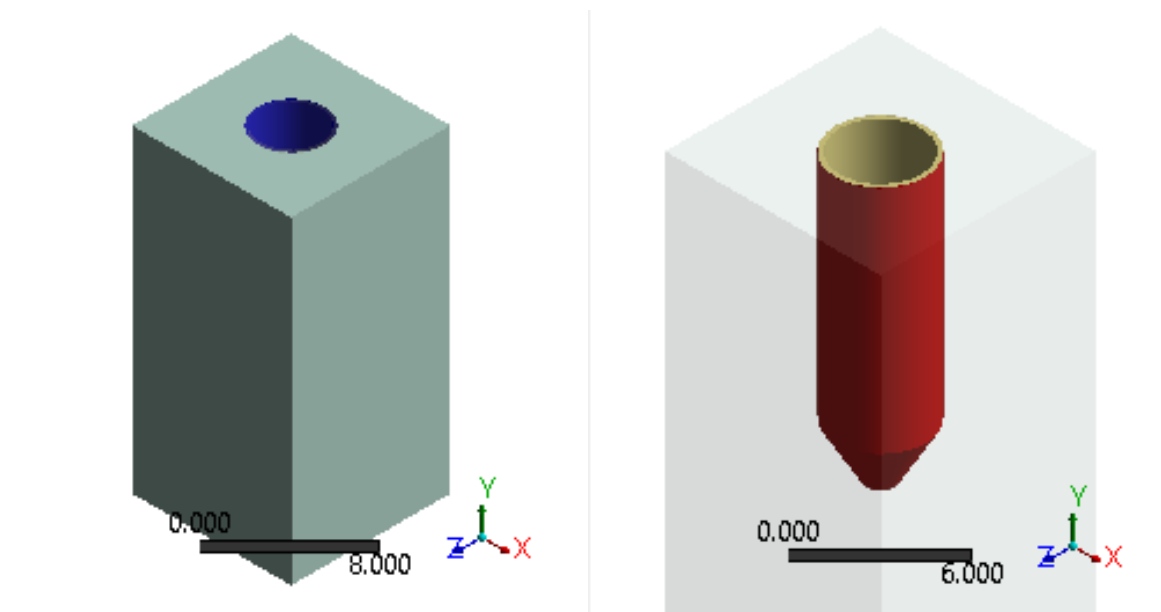


Figure A.6: Connection 6. The bone is in the left and the PDMS film on the right.

# Appendix B

# Results of Simulations
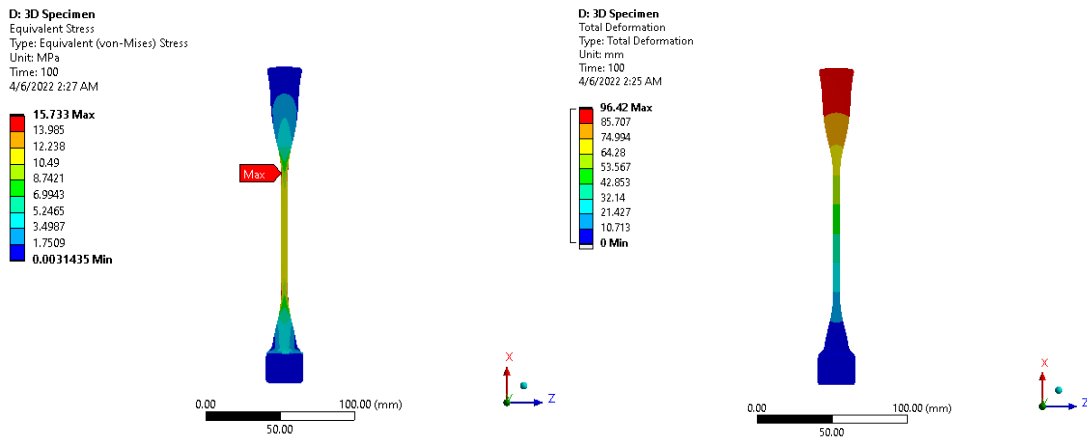
Figure B.1: Equivalent Stress and Total Deformation of the specimen.
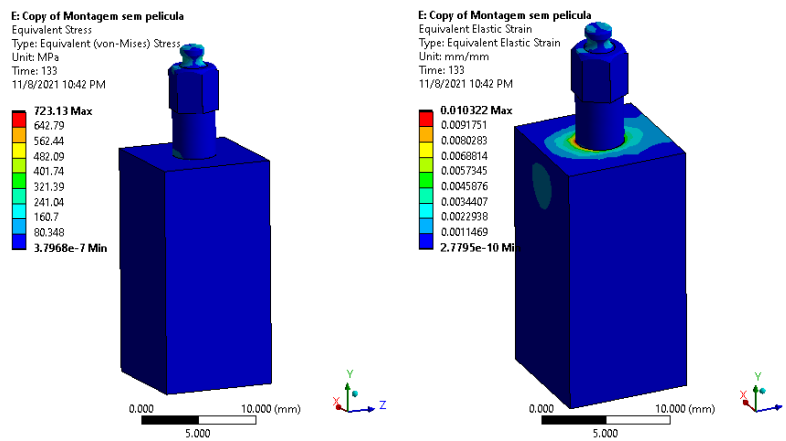


Figure B.2: Stress and Elastic Strain of the assembly without film.
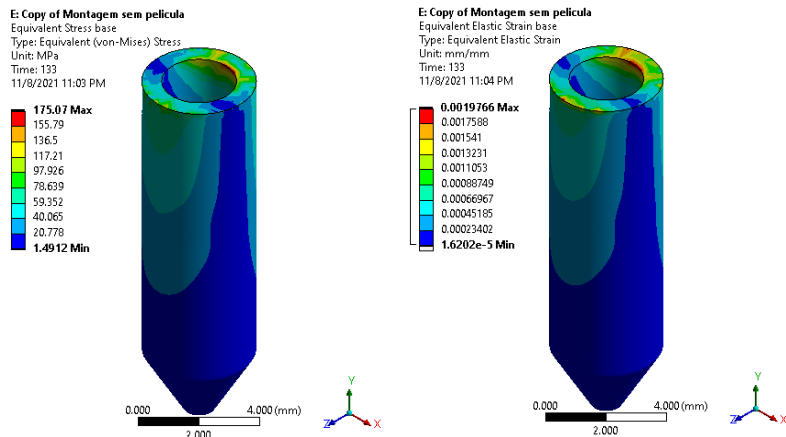


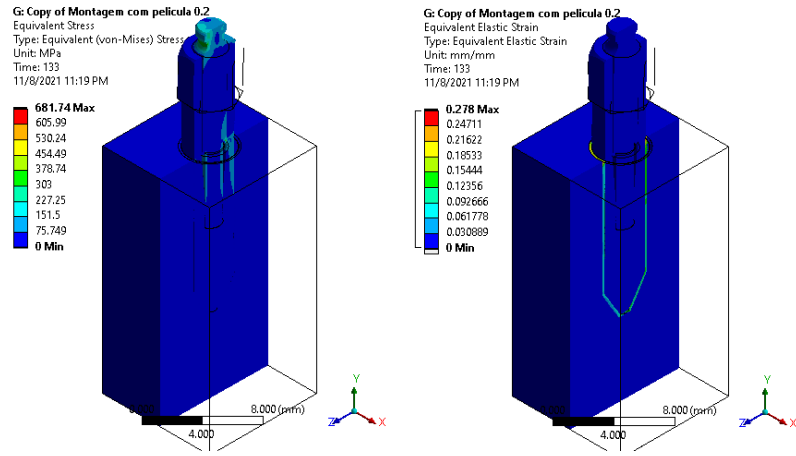Figure B.3: Stress and Elastic Strain of the screw, analysis withou film.

Figure B.4: Stress, and Elastic Strain of the assembly. Analysis with film.
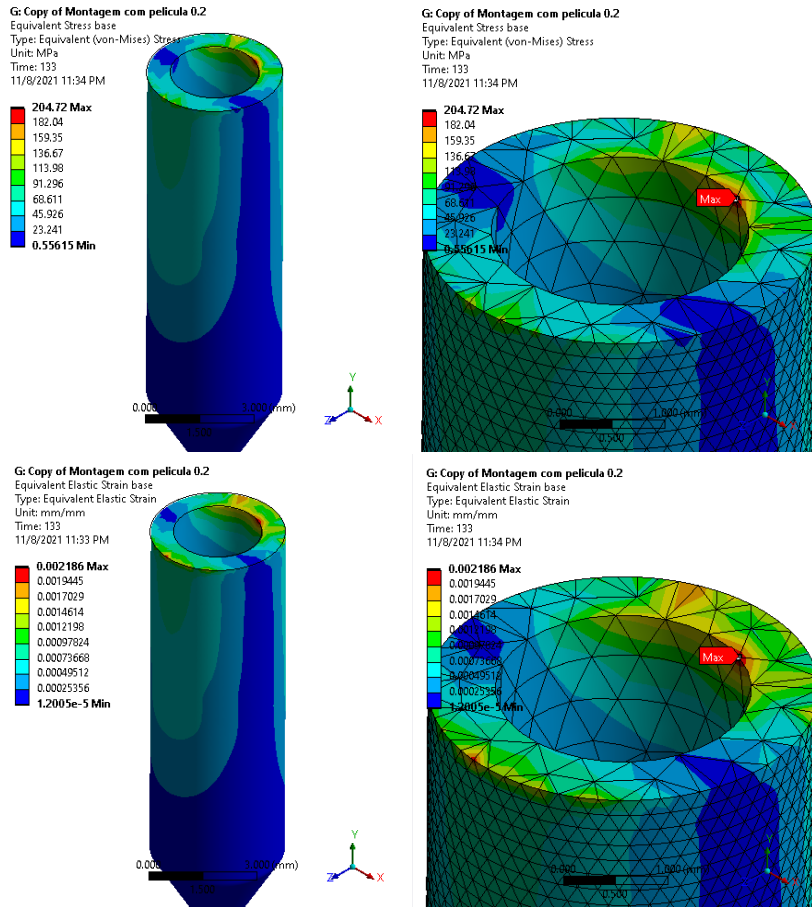


Figure B.5: Stress standard, and zoom, Elastic Strain standard, and zoom of the screw. Analysis with film.
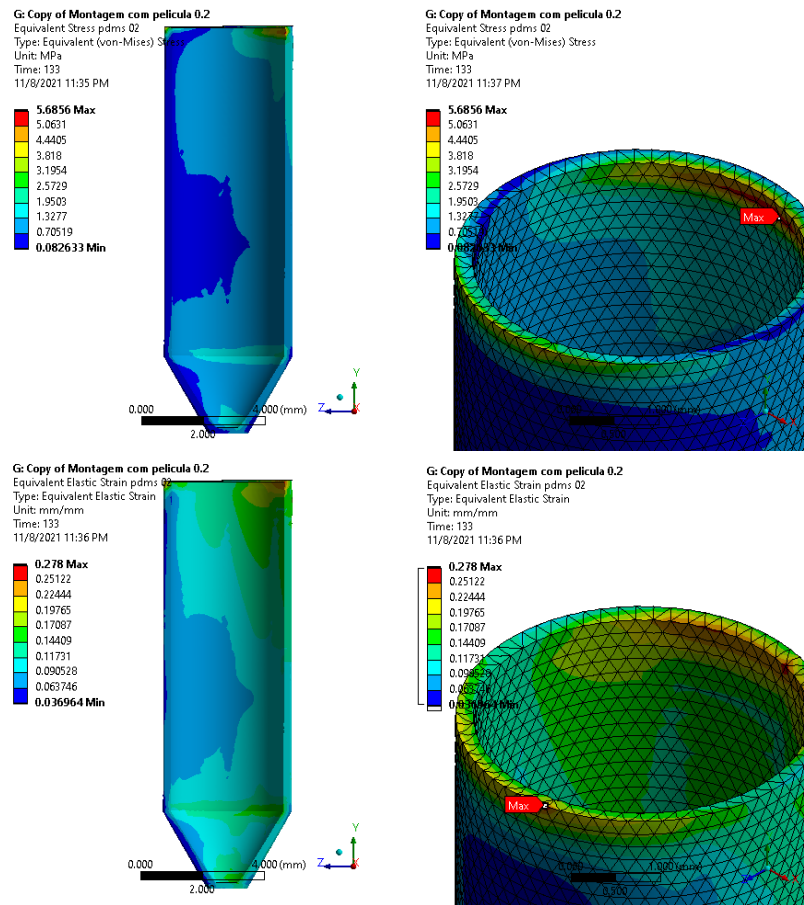
Figure B.6: Stress standard, and zoom, Elastic Strain standard, and zoom of the PDMS film. Analysis with film.
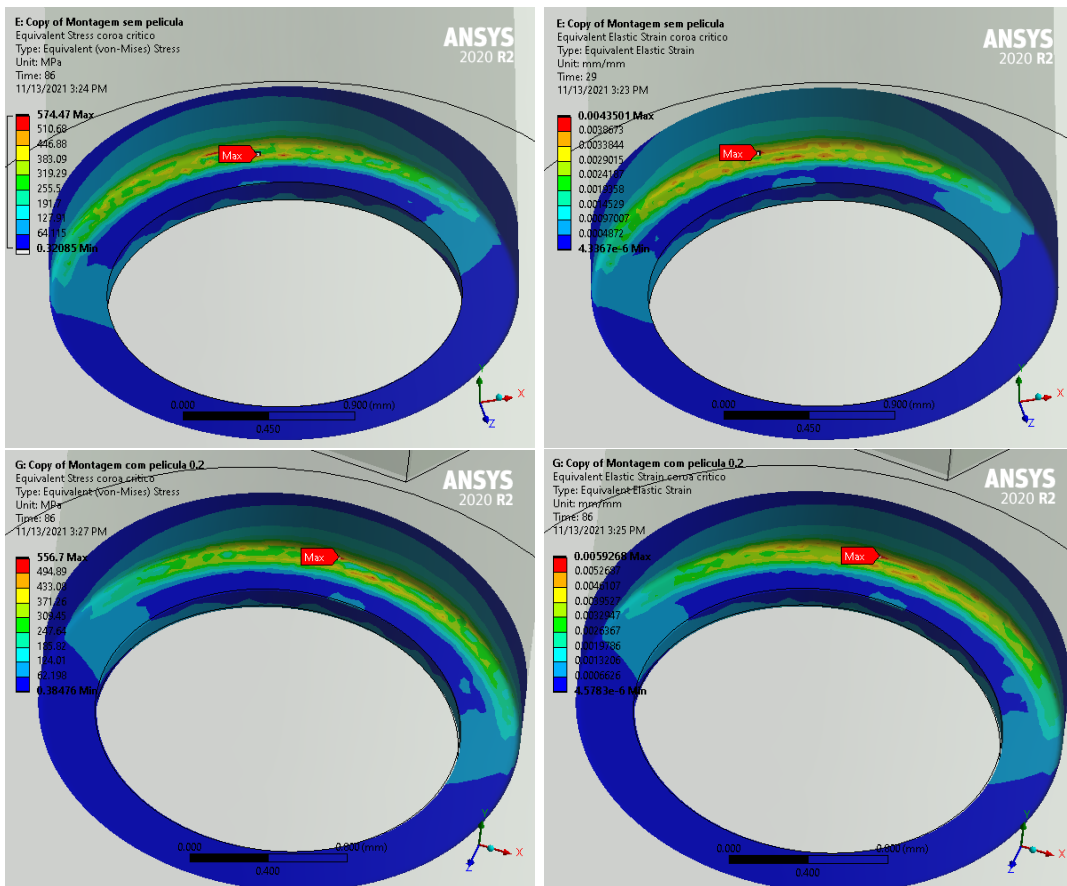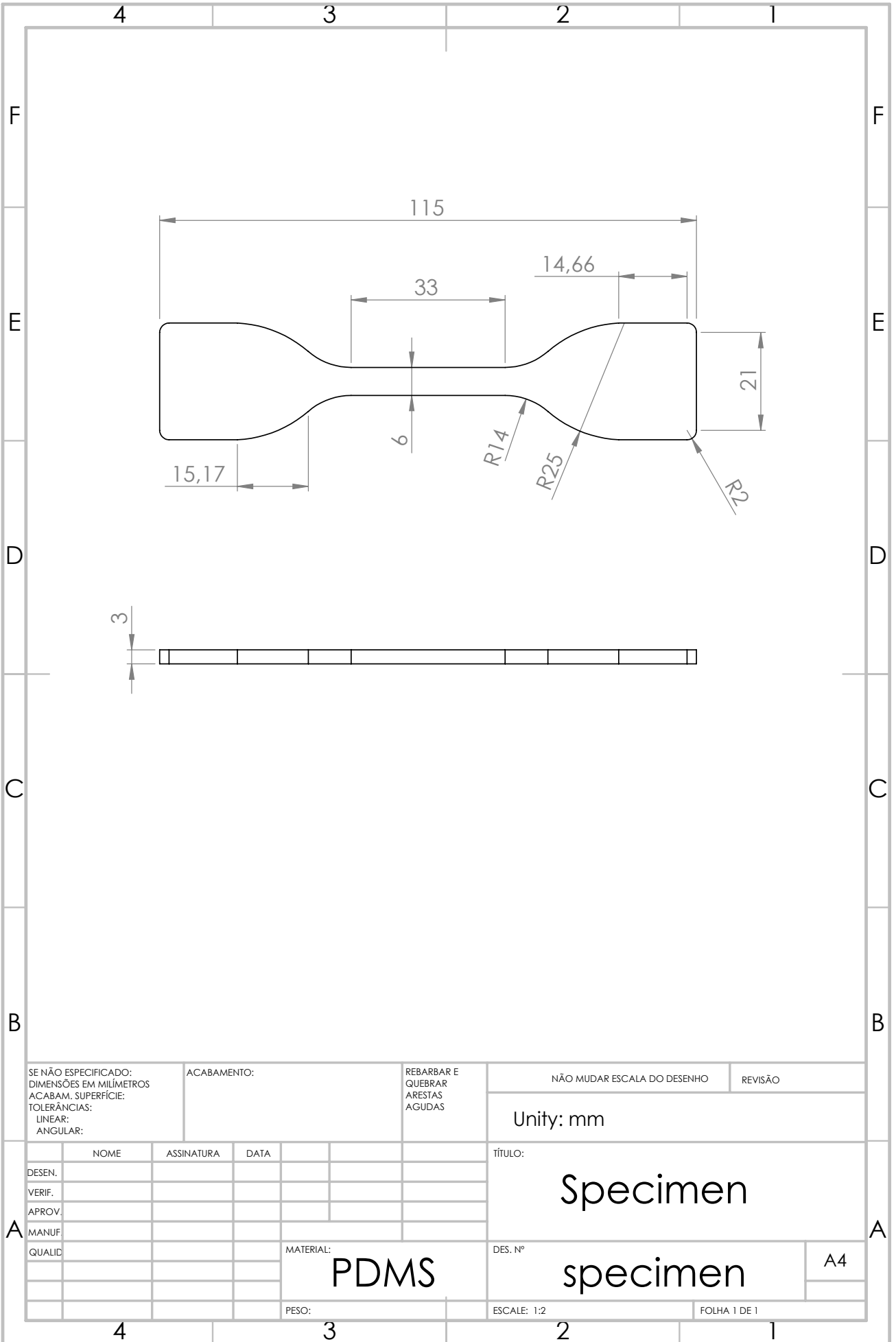
Figure B.7: Stress, and Strain of the crown without film on the top, Stress, and Strain in the crown with film on the bottom. Analysis with force 86 N.

# Appendix C

# Technical Drawing

| | 4 | 3 | 2 | 1 |

115

14,66

33

21

R14

R25

R2

6

15,17

3

| | NOME | ASSINATURA | DATA | | | TÍTULO: |

DESEN.

VERIF.

APROV.

MANUF.

QUALID

Specimen

MATERIAL:

PDMS

DES. Nº

specimen

A4

PESO:

ESCALE: 1:2

FOLHA 1 DE 1

C2

| 4 | 3 | 2 | 1 |

⌀3,75  A

10,67

2,33

30°

**Frontal View**

1,79

4,80°

2

6
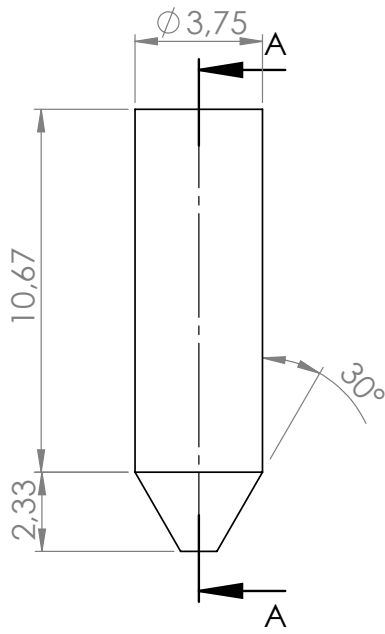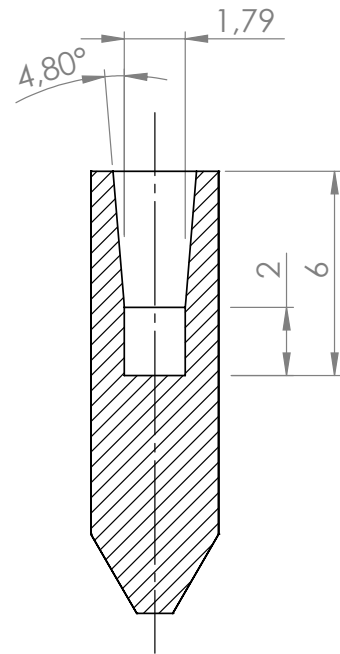
**Section A-A**

**Isometric View**

| | NOME | ASSINATURA | DATA | | | TÍTULO: |
|---|---|---|---|---|---|---|
| DESEN. | | | | | | |
| VERIF. | | | | | | **Retaining Screw** |
| APROV. | | | | | | |
| MANUF | | | | | | |
| QUALID | | | | MATERIAL:<br>**Ti 6Al-4V** | | DES. Nº  **retaining_screw**   A4 |
| | | | | PESO: | | ESCALE: 5:1   FOLHA 1 DE 1 |

| 4 | 3 | 2 | 1 |

C3

| 4 | 3 | 2 | 1 |
|---|---|---|---|

Ø1,85
Ø2,15
Ø2,38

**Superior View**

**Isometric View**

0,17x45°

R0,69

9,60

1,08

7,88

6,11

A

Ø1,79

**Frontal View**

2xR0,02

**Detail A**
**Scale 50 : 1**

| | NOME | ASSINATURA | DATA | | | | TÍTULO: |
|---|---|---|---|---|---|---|---|
| DESEN. | | | | | | | |
| VERIF. | | | | | | | **Pillar** |
| APROV. | | | | | | | |
| MANUF | | | | | | | |
| QUALID | | | | MATERIAL: | | DES. Nº | |

MATERIAL: **Ti 6Al-4V**

DES. Nº **pillar**

A4

PESO:

ESCALA:5:1

FOLHA 1 DE 1

C4

Isometric View

4,42

3,83

Ø 3,62

Ø 2,46

Ø 1,86

Superior View

R0,03

0,12

Detail E
Scale 50 : 1

B

0,40x45°

7,99

4,12

B

Superior View

E

Ø 3,83

Section B-B

| | NOME | ASSINATURA | DATA | | | TÍTULO: |
|---|---|---|---|---|---|---|
| DESEN. | | | | | | |
| VERIF. | | | | | | Crown |
| APROV. | | | | | | |
| MANUF | | | | | | |
| QUALID | | | MATERIAL: | | DES. Nº | |

Ti 6Al-4V

crown

A4

PESO:

ESCALE: 5:1

FOLHA 1 DE 1

C5

B

F

E

D

B

Frontal View

Section B-B

C

C6



Isometric View

3

2

1

| Item | Name | Quant. |
|------|------|--------|
| 1 | Retaining Screw | 1 |
| 2 | Crown | 1 |
| 3 | Pillar | 1 |